present in all the unrelated families with ARH in Sardinia and Italy. Al-Kateb *et al.* (18) reported an intron 1 acceptor splice-site mutation in the *ARH* gene in a Syrian family. They also found the 13q22-q32 locus as a gene strongly influencing LDL levels in another family with ARH and normal dizygotic twins.

In addition, we identified one single nucleotide polymorphism in the region in which an insertion mutation was found. This nucleotide substitution of cytosine by thymine at position 604 changes the coded amino acid from a proline to a serine at position 202 (*ARH-604C* and *ARH-604T*). Among 20 healthy normolipidemic volunteers, four are homozygous and 10 are heterozygous for this variation. According to a report by Garcia *et al.* (8), a mutation of cytosine to adenine at position 605 changes the coded amino acid residue from a proline to a histidine at position 202 and causes ARH. Thus, this position with eight sequential cytosines appears to be a mutation hot spot. It is noteworthy that the amino acid change from a proline to a serine at position 202 does not cause any apparent disorder, but the substitution by histidine at the same position produces severe clinical symptoms of ARH. Additional large-scale screening studies are required to identify the clinical significance of this nucleotide polymorphism.

Neither *ARH* mRNA nor protein was detected in the fibroblasts of homozygous patients. It is plausible that extreme instability of mRNA coding for ARH protein could be responsible for all clinical manifestations of the affected siblings rather than expression of the truncated protein. The phenomenon that early termination of translation caused by nonsense mutation or frame shift is called nonsense-mediated mRNA decay (19). Although the mechanism of nonsense-mediated mRNA decay has not been fully explained, this phenomenon is universally observed in yeast, plants, and mammals (19). We have previously reported such a mutation in LPL deficiency family who had a one-base deletion in exon 5 of the *LPL* gene resulting in premature termination by frame shift (20).

The function of the protein encoded by *ARH* needs to be clarified. The amount of LDL receptor mRNA is normal, and the receptor protein functions normally in the fibroblasts of homozygote patients in a cell culture system. This includes binding, internalization, and degradation of LDL (3). However, homozygous mutations of *ARH* result in the symptoms apparently similar to homozygous FH. The retarded turnover of LDL in the patients' plasma strongly indicates that the product of *ARH* modulates clearance of plasma LDL. Thus, ARH putatively alters the function of the LDL receptor *in vivo*, especially in the liver because 80% of human plasma LDL is cleared in the liver (21). Garcia *et al.* (8) suggested that *ARH* encodes a putative LDL receptor adaptor protein and may participate in the regulation of localization of the LDL receptor in polarized cells. The PTB domain of *ARH* is considered to interact with the cytoplasmic tail of the LDL receptor, which is required for trafficking of the LDL receptor to the basolateral surface (22, 23). In fact, mutation of the cytoplasmic domain of the LDL receptor results in its misdirected targeting to the apical surface in hepatic epithelial cells (24). Recently, He *et al.* (25) reported that ARH interacts with LDL receptor, clathrin, and adaptor protein complex 2 and may play a role in endocytosis. The precise roles of ARH on LDL receptor protein remain to be elucidated.

In addition, both patients were found to have fatty livers, which has never been described either for FH or ARH. They were diagnosed with the fatty liver at around the age of 30 yr despite not having any of the common causes of this disorder such as obesity, hyperinsulinemia, alcoholism, or the use of specific drugs. Therefore, this finding may also be associated with the mutation of *ARH* and the function of the product of this gene may be related to regulation of intracellular lipid metabolism, although we cannot exclude the possibility of mere coincidence.

Here, we report homozygous patients with ARH, who have a novel insertion mutation in the *ARH* gene. A putative major single nucleotide polymorphism has also been identified at this region of *ARH*.

Acknowledgments

We thank Drs. Kenji Kangawa, Hisayuki Matsuo, and Yasunao Yoshimasa for helpful discussion and advice; Dr. Yoshitane Tsukamoto for taking the histological pictures; and Dr. Patrick Leahy for proofreading this manuscript. We also thank Keiko Jinno, Eri Abe, and Moto Ohira for excellent technical assistance.

Received September 23, 2002. Accepted November 20, 2002.

Address all correspondence and requests for reprints to: Dr. Mariko Harada-Shiba, Department of Bioscience, National Cardiovascular Center Research Institute, Fujishiro-dai, Suita, Osaka 565-8565, Japan. E-mail: mshiba@ri.ncvc.go.jp.

This work was supported in part by the Promotion of Fundamental Studies in Health Science of the Organization for Pharmaceutical Safety and Research (OPSR); Setsuro Fujii Memorial, the Osaka Foundation for Promotion of Fundamental Medical Research; and a Grant-in-Aid for Scientific Research (C) (no. 12670384) from the Ministry of Education, Science, Sports, and Culture, Japan.

References

1. **Khachadurian AK, Uthman SM** 1973 Experiences with the homozygous cases of familial hypercholesterolemia. A report of 52 patients. Nutr Metab 15: 132–140
2. **Goldstein JL, Hobbs HH, Brown MS** 2001 Familial hypercholesterolemia. In: Scriver CR, Beaudet AL, Sly WS, Valle D, eds. The metabolic and molecular bases of inherited disease, ed 8, vol 2. New York: McGraw-Hill; 2863–2913
3. **Harada-Shiba M, Tajima S, Miyake Y, Kojima S, Tsushima M, Yamamoto A** 1991 Severe hypercholesterolemia patients with normal LDL receptor. J Jpn Atheroscler Soc 19:227–242
4. **Harada-Shiba M, Tajima S, Yokoyama S, Miyake Y, Kojima S, Tsushima M, Kawakami M, Yamamoto A** 1992 Siblings with normal LDL receptor activity and severe hypercholesterolemia. Arterioscler Thromb 12:1071–1078
5. **Zuliani G, Vigna GB, Corsini A, Maioli M, Romagnoni F, Fellin R** 1995 Severe hypercholesterolaemia: unusual inheritance in an Italian pedigree. Eur J Clin Invest 25:322–331
6. **Schmidt HH, Stuhrmann M, Shamburek R, Schewe CK, Ebhardt M, Zech LA, Buttner C, Wendt M, Beisiegel U, Brewer Jr HB, Manns MP** 1998 Delayed low density lipoprotein (LDL) catabolism despite a functional intact LDL-apolipoprotein B particle and LDL-receptor in a subject with clinical homozygous familial hypercholesterolemia. J Clin Endocrinol Metab 83:2167–2174
7. **Zuliani G, Arca M, Signore A, Bader G, Fazio S, Chianelli M, Bellosta S, Campagna F, Montali A, Maioli M, Pacifico A, Ricci G, Fellin R** 1999 Characterization of a new form of inherited hypercholesterolemia: familial recessive hypercholesterolemia. Arterioscler Thromb Vasc Biol 19:802–809
8. **Garcia CK, Wilund K, Arca M, Zuliani G, Fellin R, Maioli M, Calandra S. Bertolini S, Cossu F, Grishin N, Barnes R, Cohen JC, Hobbs HH** 2001 Autosomal recessive hypercholesterolemia caused by mutations in a putative LDL receptor adaptor protein. Science 292:1394–1398
9. **Chomczynski P, Sacchi N** 1987 Single-step method of RNA isolation by acid guanidinium thiocyanate-phenol-chloroform extraction. Anal Biochem 162: 156–159
10. **Feinberg AP, Vogelstein B** 1983 A technique for radiolabeling DNA restriction endonuclease fragments to high specific activity. Anal Biochem 132:6–13
11. **Venter JC, Adams MD, Myers EW, Li PW, Mural RJ, Sutton GG, Smith HO,**

Yandell M, Evans CA, Holt RA, Gocayne JD, Amanatides P, Ballew RM, Huson DH, Wortman JR, Zhang Q, Kodira CD, Zheng XH, Chen L, Skupski M, Subramanian G, Thomas PD, Zhang J, Gabor Miklos GL, Nelson C, Broder S, Clark AG, Nadeau J, McKusick VA, Zinder N, Levine AJ, Roberts RJ, Simon M, Slayman C, Hunkapiller M, Bolanos R, Delcher A, Dew I, Fasulo D, Flanigan M, Florea L, Halpern A, Hannenhalli S, Kravitz S, Levy S, Mobarry C, Reinert K, Remington K, Abu-Threideh J, Beasley E, Biddick K, Bonazzi V, Brandon R, Cargill M, Chandramouliswaran I, Charlab R, Chaturvedi K, Deng Z, Di Francesco V, Dunn P, Eilbeck K, Evangelista C, Gabrielian AE, Gan W, Ge W, Gong F, Gu Z, Guan P, Heiman TJ, Higgins ME, Ji RR, Ke Z, Ketchum KA, Lai Z, Lei Y, Li Z, Li J, Liang Y, Lin X, Lu F, Merkulov GV, Milshina N, Moore HM, Naik AK, Narayan VA, Neelam B, Nusskern D, Rusch DB, Salzberg S, Shao W, Shue B, Sun J, Wang Z, Wang A, Wang X, Wang J, Wei M, Wides R, Xiao C, Yan C, Yao A, Ye J, Zhan M, Zhang W, Zhang H, Zhao Q, Zheng L, Zhong F, Zhong W, Zhu S, Zhao S, Gilbert D, Baumhueter S, Spier G, Carter C, Cravchik A, Woodage T, Ali F, An H, Awe A, Baldwin D, Baden H, Barnstead M, Barrow I, Beeson K, Busam D, Carver A, Center A, Cheng ML, Curry L, Danaher S, Davenport L, Desilets R, Dietz S, Dodson K, Doup L, Ferriera S, Garg N, Gluecksmann A, Hart B, Haynes J, Haynes C, Heiner C, Hladun S, Hostin D, Houck J, Howland T, Ibegwam C, Johnson J, Kalush F, Kline L, Koduru S, Love A, Mann F, May D, McCawley S, McIntosh T, McMullen I, Moy M, Moy L, Murphy B, Nelson K, Pfannkoch C, Pratts E, Puri V, Qureshi H, Reardon M, Rodriguez R, Rogers YH, Romblad D, Ruhfel B, Scott R, Sitter C, Smallwood M, Stewart E, Strong R, Suh E, Thomas R, Tint NN, Tse S, Vech C, Wang G, Wetter J, Williams S, Williams M, Windsor S, Winn-Deen E, Wolfe K, Zaveri J, Zaveri K, Abril JF, Guigo R, Campbell MJ, Sjolander KV, Karlak B, Kejariwal A, Mi H, Lazareva B, Hatton T, Narechania A, Diemer K, Muruganujan A, Guo N, Sato S, Bafna V, Istrail S, Lippert R, Schwartz R, Walenz B, Yooseph S, Allen D, Basu A, Baxendale J, Blick L, Caminha M, Carnes-Stine J, Caulk P, Chiang YH, Coyne M, Dahlke C, Mays A, Dombroski M, Donnelly M, Ely D, Esparham S, Fosler C, Gire H, Glanowski S, Glasser K, Glodek A, Gorokhov M, Graham K, Gropman B, Harris M, Heil J, Henderson S, Hoover J, Jennings D, Jordan C, Jordan J, Kasha J, Kagan L, Kraft C, Levitsky A, Lewis M, Liu X, Lopez J, Ma D, Majoros W, McDaniel J, Murphy S, Newman M, Nguyen T, Nguyen N, Nodell M, Pan S, Peck J, Peterson M, Rowe W, Sanders R, Scott J, Simpson M, Smith T, Sprague A, Stockwell T, Turner R, Venter E, Wang M, Wen M, Wu D, Wu M, Xia A, Zandieh A, Zhu X 2001 The sequence of the human genome. Science 291:1304–1351

12. **Folch J, Lees M, Sloane SGH** 1957 A simple method for the isolation and purification of total lipids from animal tissues. J Biol Chem 226:497–509
13. **Lehnus G, Smith L** 1978 Automated procedure for kinetic measurement of total triglycerides (as glycerol) in serum with the Gilford System 3500. Clin Chem 24:27–31
14. **Richmond W** 1973 Preparation and properties of a cholesterol oxidase from Nocardia sp. and its application to the enzymatic assay of total cholesterol in serum. Clin Chem 19:1350–1356
15. **Takayama M, Itoh S, Nagasaki T, Tanimizu I** 1977 A new enzymatic method for determination of serum choline-containing phospholipids. Clin Chim Acta 79:93–98
16. **Adachi S, Ishiba M, Isozaki A, Yamamoto A, Kakiuchi Y, Shingi Y** 1970 Lipid analysis of the biopsy specimen of the liver. Jpn J Gastroenterol 67:332–342
17. **Arca M, Zuliani G, Wilund K, Campagna F, Fellin R, Bertolini S, Calandra S, Ricci G, Glorioso N, Maioli M, Pintus P, Carru C, Cossu F, Cohen J, Hobbs HH** 2002 Autosomal recessive hypercholesterolemia in Sardinia, Italy, and mutations in *ARH*: a clinical and molecular genetic analysis. Lancet 359:841–847
18. **Al-Kateb H, Bähring S, Hoffmann K, Strauch K, Busjahn A, Nurnberg G, Jouma M, Bautz EKF, Dresel HA, Luft FC** 2002 Mutation in the ARH gene and a chromosome 13q locus influence cholesterol levels in a new form of digenic-recessive familial hypercholesterolemia. Circ Res 90:951–958
19. **Ross J** 1995 mRNA stability in mammalian cells. Microbiol Rev 59:423–450
20. **Takagi A, Ikeda Y, Tsutsumi Z, Shoji T, Yamamoto A** 1992 Molecular studies on primary lipoprotein lipase (LPL) deficiency. One base deletion (G916) in exon 5 of LPL gene causes no detectable LPL protein due to the absence of LPL mRNA transcript. J Clin Invest 89:581–591
21. **Bilheimer DW** 1989 Portacaval shunt and liver transplantation in treatment of familial hypercholesterolemia. Arteriosclerosis 9(Suppl 1):I158–I163
22. **Matter K, Hunziker W, Mellman I** 1992 Basolateral sorting of LDL receptor in MDCK cells: the cytoplasmic domain contains two tyrosine-dependent targeting determinants. Cell 71:741–753
23. **Yokode M, Pathak RK, Hammer RE, Brown MS, Goldstein JL, Anderson RG** 1992 Cytoplasmic sequence required for basolateral targeting of LDL receptor in livers of transgenic mice. J Cell Biol 117:39–46
24. **Koivisto UM, Hubbard AL, Mellman I** 2001 A novel cellular phenotype for familial hypercholesterolemia due to a defect in polarized targeting of LDL receptor. Cell 105:575–585
25. **He G, Gupta S, Yi M, Michaely P, Hobbs HH, Cohen JC** 2002 ARH is a modular adaptor protein that interacts with the LDL receptor, clathrin and AP-2. J Biol Chem 277:44044–44049

Hybrid Cell–Gene Therapy for Pulmonary Hypertension Based on Phagocytosing Action of Endothelial Progenitor Cells

Noritoshi Nagaya, MD; Kenji Kangawa, PhD; Munetake Kanda, MD; Masaaki Uematsu, MD; Takeshi Horio, MD; Naoto Fukuyama, MD; Jun Hino, PhD; Mariko Harada-Shiba, MD; Hiroyuki Okumura, MD; Yasuhiko Tabata, PhD; Naoki Mochizuki, MD; Yoshihide Chiba, MD; Keisuke Nishioka, MD; Kunio Miyatake, MD; Takayuki Asahara, MD; Hiroshi Hara, MD; Hidezo Mori, MD

Background—Circulating endothelial progenitor cells (EPCs) migrate to injured vascular endothelium and differentiate into mature endothelial cells. We investigated whether transplantation of vasodilator gene-transduced EPCs ameliorates monocrotaline (MCT)-induced pulmonary hypertension in rats.

Methods and Results—We obtained EPCs from cultured human umbilical cord blood mononuclear cells and constructed plasmid DNA of adrenomedullin (AM), a potent vasodilator peptide. We used cationic gelatin to produce ionically linked DNA-gelatin complexes. Interestingly, EPCs phagocytosed plasmid DNA-gelatin complexes, which allowed nonviral, highly efficient gene transfer into EPCs. Intravenously administered EPCs were incorporated into the pulmonary vasculature of immunodeficient nude rats given MCT. Transplantation of EPCs alone modestly attenuated MCT-induced pulmonary hypertension (16% decrease in pulmonary vascular resistance). Furthermore, transplantation of AM DNA-transduced EPCs markedly ameliorated pulmonary hypertension in MCT rats (39% decrease in pulmonary vascular resistance). MCT rats transplanted with AM-expressing EPCs had a significantly higher survival rate than those given culture medium or EPCs alone.

Conclusions—Umbilical cord blood–derived EPCs had a phagocytosing action that allowed nonviral, highly efficient gene transfer into EPCs. Transplantation of AM gene-transduced EPCs caused significantly greater improvement in pulmonary hypertension in MCT rats than transplantation of EPCs alone. Thus, a novel hybrid cell–gene therapy based on the phagocytosing action of EPCs may be a new therapeutic strategy for the treatment of pulmonary hypertension. **(*Circulation*. 2003;108:889-895.)**

Key Words: pulmonary heart disease ■ natriuretic peptides ■ gene therapy ■ endothelium

The pulmonary endothelium plays an important role in the regulation of pulmonary vascular tone through the release of vasoactive substances such as nitric oxide, prostacyclin, and adrenomedullin (AM).[1] Dysfunction of the endothelium may play a role in the pathogenesis of pulmonary hypertension, including primary pulmonary hypertension.[2] Thus, pulmonary endothelial cells may be a therapeutic target for the treatment of pulmonary hypertension. Recently, endothelial progenitor cells (EPCs) have been discovered in adult peripheral blood.[3] EPCs are mobilized from bone marrow into the peripheral blood in response to tissue ischemia or traumatic injury, migrate to sites of injured endothelium, and differentiate into mature endothelial cells in situ.[4–6] These findings raise the possibility that transplanted EPCs may serve not only as a tissue-engineering tool to reconstruct the pulmonary vasculature but also as a vehicle for gene delivery to injured pulmonary endothelium.

We prepared biodegradable gelatin that could hold negatively charged protein or plasmid DNA in its positively charged lattice structure.[7,8] We have shown that the gelatin is promptly phagocytosed and then gradually degraded by phagocytes, including macrophages.[9] However, whether EPCs phagocytose ionically linked plasmid DNA-gelatin complexes remains unknown. If this is the case, the phago-

Received December 3, 2002; revision received April 17, 2003; accepted April 18, 2003.

From the Departments of Internal Medicine (N.N., T.H., K.M.) and Perinatology (Y.C.), National Cardiovascular Center, Osaka, Japan; Departments of Biochemistry (K.K., J.H., M.H.-S., H.O.), Cardiac Physiology (M.K., H.M.), and Structural Analysis (N.M.), National Cardiovascular Center Research Institute, Osaka, Japan; Cardiovascular Division (M.U.), Kansai Rosai Hospital, Hyogo, Japan; Department of Physiology (N.F.), Tokai University School of Medicine, Kanagawa, Japan; Department of Biomaterials (Y.T.), Field of Tissue Engineering, Institute for Frontier Medical Sciences, Kyoto University, Kyoto, Japan; Department of Transfusion Medicine (K.N., H.H.), Hyogo College of Medicine, Hyogo, Japan; and Department of Regenerative Medicine (T.A.), Institute of Biomedical Research and Innovation, Kobe, Japan.

Reprint requests to Noritoshi Nagaya, MD, or Hidezo Mori, MD, Department of Internal Medicine, National Cardiovascular Center, 5-7-1 Fujishirodai, Suita, Osaka 565-8565, Japan. E-mail nagayann@hsp.ncvc.go.jp or hidemori@ri.ncvc.go.jp

Circulation is available at http://www.circulationaha.org

DOI: 10.1161/01.CIR.0000079161.56080.22

cytic activity of EPCs would allow nonviral gene transfer into EPCs. Here we provide rationale of a novel hybrid cell–gene therapy for pulmonary hypertension.

AM is a potent vasodilator peptide that was originally isolated from human pheochromocytoma.[1] There are abundant binding sites for AM in the pulmonary vasculature.[10] The plasma AM level increases in proportion to the severity of pulmonary hypertension, and circulating AM is partially metabolized in the lungs.[11] Recently, we have shown that intravenous administration of AM significantly decreases pulmonary vascular resistance in patients with heart failure or primary pulmonary hypertension.[12,13] These findings suggest that AM plays an important role in the regulation of pulmonary vascular tone. Thus, we hypothesized that transplantation of AM DNA-transduced EPCs would improve monocrotaline (MCT)-induced pulmonary hypertension. To test this hypothesis, we investigated whether EPCs phagocytose DNA-gelatin complexes, which would allow nonviral gene transfer into EPCs; whether intravenously administered EPCs are incorporated into the pulmonary vasculature; and whether transplantation of AM DNA-transduced EPCs ameliorates MCT-induced pulmonary hypertension and improves survival in MCT rats.

Methods

Culture of EPCs

Human umbilical cord blood mononuclear cells were plated on fibronectin-coated dishes and cultured in Medium 199 supplemented with 20% FBS, bovine pituitary extract, vascular endothelial growth factor, basic fibroblast growth factor, heparin, and antibiotics, as reported previously.[3,6,14] On days 4 and 8 of culture, nonadherent cells were removed, and medium was replaced. All mothers gave written informed consent, and the study was approved by the ethics committee.

Fluorescent Staining for EPCs

Adherent cells on day 8 of culture were stained by acetylated LDL labeled with DiI (DiI-acLDL, Biomedical Technologies) and fluorescein isothiocyanate (FITC)-labeled lectin from ulex europaeus (Sigma). Double-positive cells for DiI-acLDL and FITC-labeled lectin were identified as EPCs, as reported previously.[15,16]

Flow Cytometry

Adherent cells on day 8 of culture and green fluorescent protein (GFP) gene-transduced cells were analyzed by fluorescence-activated cell sorting (FACS; FACS SCAN flow cytometer, Becton Dickinson). Cells were incubated for 30 minutes at 4°C with phycoerythrin-conjugated mouse monoclonal antibodies against human CD14 (clone M5E2), CD31 (clone L133.1), CD68 (clone Y1/82A), and CD83 (clone HB15e; all from Becton Dickinson) and mouse monoclonal antibodies against human KDR (clone KDR-1, Sigma) and VE-cadherin (clone BV6, Chemicon). Isotype-identical antibodies served as controls.

Preparation of Biodegradable Gelatin and Plasmid DNA

We prepared biodegradable cationic gelatin, as a matrix to hold plasmid DNA, as reported previously.[7] In brief, a gelatin sample with an isoelectric point of 9.0 was isolated from bovine bone collagen. Gelatin microspheres were prepared through the glutaraldehyde cross-linking of gelatin. The microspheres were washed with acetone and distilled water and then freeze-dried. We constructed the pcDNA1.1-CMV vector (Invitrogen) encoding human AM cDNA or GFP cDNA. The gelatin (5 to 30 μm in diameter, 2 mg) was added to plasmid DNA (200 μg/200 μL in PBS, pH 7.4). After 24-hour incubation at 4°C, DNA-gelatin complexes were obtained.

Ex Vivo Gene Transfer Into EPCs

EPCs (5×10^5) were cultured with ionically linked GFP or AM DNA-gelatin complexes (200 μg/2 mg) for 72 hours. To examine DNA localization, AM plasmid DNA was labeled by rhodamine B isothiocyanate (RITC), as reported previously.[8] The nuclei of EPCs were stained by DAPI (Sigma). Immunocytochemistry for AM was performed with a mouse monoclonal antibody against human AM-(46-52). Human AM level in culture medium (n=5) was measured by radioimmunoassay.

Assay for AM

The culture medium and lung tissues were acidified with acetic acid, boiled to inactivate intrinsic proteases, and lyophilized. Human AM levels in culture medium, lung tissues, and plasma were measured with a radioimmunoassay kit (Shionogi).[12]

In Vivo Experimental Protocol

Male immunodeficient (F344/N rnu/rnu) nude rats weighing 100 to 120 g were randomly assigned to receive a subcutaneous injection of 60 mg/kg MCT or 0.9% saline. Seven days after MCT injection, 1×10^6 EPCs, 1×10^6 AM-expressing EPCs, or culture medium (500 μL each) was administered intravenously via the left jugular vein. Sham rats also received intravenous administration of 500 μL of culture medium. We used 1×10^6 cells per rat to obtain maximal effects of transplanted EPCs on the basis of dose-response experiments. This protocol resulted in the creation of 4 groups: MCT rats given EPCs (EPC group, n=8), MCT rats given AM-expressing EPCs (AM-EPC group, n=9), MCT rats given culture medium (control group, n=9), and sham rats given culture medium (sham group, n=8). Human mature pulmonary artery endothelial cells served as control cells.

Hemodynamic studies were performed 3 weeks after MCT injection. A polyethylene catheter was inserted into the right femoral artery. An umbilical vessel catheter was inserted through the right jugular vein into the pulmonary artery. Cardiac output was measured in triplicate by the thermodilution method. Pulmonary vascular resistance was calculated by dividing mean pulmonary arterial pressure by cardiac output.

Immunohistochemical and Immunofluorescence Staining

Immunohistochemistry was performed on paraformaldehyde-fixed, paraffin-embedded 5-μm sections of the lungs. To discern human endothelial cells from rat cells, we used mouse anti-human CD31 (DAKO) and mouse anti-rat CD31 (BD PharMingen) monoclonal antibodies. The sections were sequentially developed for the peroxidase and alkaline phosphatase substrates. Immunofluorescence staining for rat CD31 was performed on frozen sections with mouse anti-rat CD31 monoclonal antibody (BD PharMingen) and RITC-conjugated anti-mouse IgG antibody (DAKO).

Morphometric Analysis of Pulmonary Arteries

We analyzed the medial wall thickness of the pulmonary arteries in the middle region of the right lung (20 muscular arteries/rat, ranging in external diameter from 25 to 50 and from 51 to 100 μm). The medial wall thickness was expressed as follows: % wall thickness=[(medial thickness×2)/external diameter]×100.

Survival Analysis

Seven days after MCT injection, 29 rats received intravenous injection of 1×10^6 EPCs (EPC group, n=10), 1×10^6 AM-expressing EPCs (AM-EPC group, n=10), or culture medium (control group, n=9). Survival was estimated from the date of MCT injection to the death of the rat or 10 weeks after transplantation.

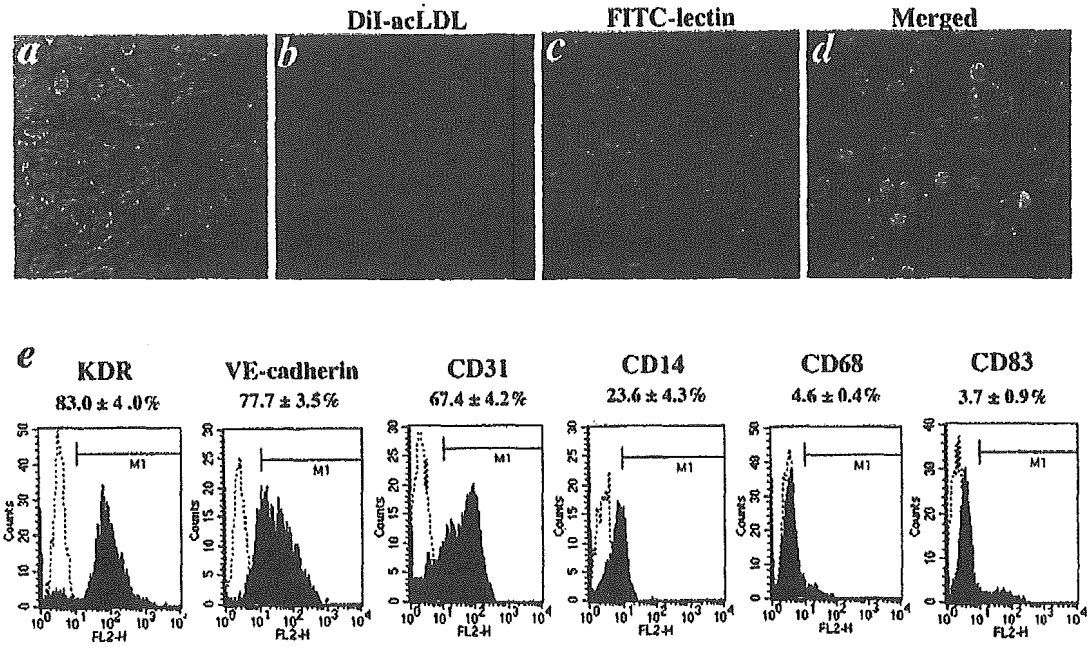

Figure 1. Characterization of EPCs derived from human umbilical cord blood. EPCs exhibited spindle-shaped or cobblestone-like morphology (a) and took up Dil-acLDL and FITC-labeled lectin in same field (b–d). e, Flow cytometric analysis of adherent cells on day 8. Most of adherent cells expressed endothelial lineage markers (KDR, VE-cadherin, and CD31), whereas they were negative for CD68 and CD83.

Statistical Analysis

Data were expressed as mean±SEM. Comparisons of parameters among the 4 groups were made by 1-way ANOVA, followed by the Scheffe multiple comparison test. Comparisons of the time course of parameters between the 2 groups were made by 2-way ANOVA for repeated measures, followed by the Scheffe multiple comparison test. Survival curves were derived by the Kaplan-Meier method and compared with log-rank tests. A probability value <0.05 was considered statistically significant.

Results

EPCs From Human Umbilical Cord Blood

After 8-day culture of mononuclear cells, spindle-shaped or cobblestone-like adherent cells were observed (Figure 1a). Most of the adherent cells were double stained by Dil-acLDL and FITC-labeled lectin (Figure 1b, c, and d). These cells expressed endothelial cell–specific antigens (KDR, VE-cadherin, and CD31; Figure 1e). In contrast, the majority of adherent cells were negative for monocyte/macrophage marker CD68 and dendritic cell marker CD83. Although a small fraction of the adherent cells expressed monocyte marker CD14, this marker has been shown to also be expressed on activated endothelial cells and cultured EPCs.[17] Thus, we confirmed that the major population of the adherent cells were EPCs.

Phagocytosis of DNA-Gelatin Complex by EPCs

EPCs were cultured with GFP DNA-gelatin complexes (Figure 2a). Interestingly, GFP was expressed in EPCs after 72-hour incubation (Figure 2b). Quantitative analyses by FACS confirmed a high incidence (76±3%, n=5) of GFP expression in adherent cells. KDR/GFP double-positive cells made up 70±2% of the adherent cells, whereas CD68/GFP double-positive cells accounted for 2±1% (Figure 2c). Transmission electron microscopy demonstrated that EPCs were phagocytosing DNA-gelatin complexes (Figure 2d). These results suggest that EPCs phagocytose DNA-gelatin complexes in coculture, which allows nonviral, highly efficient gene transfer into EPCs. Unlike gelatin, cationic liposome-mediated transfection efficiency was low (24±3%).

A number of DNA particles labeled by RITC were incorporated into gelatin (Figure 2e). RITC-labeled DNA particles were gradually released from gelatin within EPCs through gelatin degradation (Figure 2f). After 72-hour incubation, RITC-labeled DNA particles released from gelatin were distributed in the cytoplasm of EPCs (Figure 2g). These results suggest the ability of EPCs to take up DNA-gelatin complexes and dissolve the gelatin, freeing the DNA into EPCs. Unlike EPCs, human mature pulmonary artery endothelial cells did not phagocytose DNA-gelatin complexes.

When EPCs were cultured with AM DNA-gelatin complexes, intense immunostaining for AM was observed in EPCs impregnated with AM DNA-gelatin (Figure 3a). After 72-hour incubation, EPCs markedly secreted AM into the culture medium (10-fold increase compared with EPCs alone; Figure 3b). AM overproduction lasted for more than 16 days after gene transfer. AM secretion from EPCs was not influenced by the presence of gelatin (data not shown).

Incorporation of EPCs Into the Pulmonary Vasculature

GFP-expressing EPCs were administered intravenously 7 days after MCT injection. Three days after transplantation,

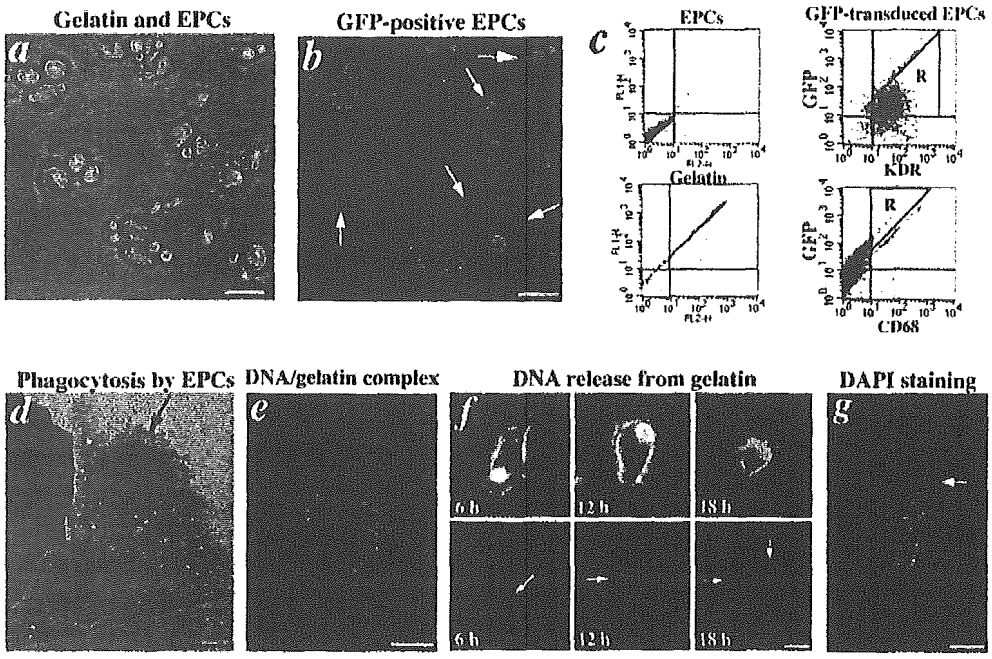

Figure 2. Ex vivo gene transfer into EPCs based on phagocytosing action. a, EPCs were cultured with ionically linked GFP DNA-gelatin complexes. b, GFP was highly expressed in EPCs (arrows) in same field as Figure 2a. c, Flow cytometric analyses of EPCs cultured with GFP DNA-gelatin complexes. Negative controls (EPC isocontrol and gelatin background) are shown in left panels. d, Transmission electron microscopy revealed that EPCs had phagocytosed GFP DNA-gelatin complexes (arrows). e, RITC-labeled DNA particles were incorporated into gelatin. f, RITC-labeled DNA particles (red, arrows) were released from gelatin through its degradation. g, RITC-labeled DNA particles released from gelatin (arrow) were distributed in cytoplasm of EPCs. Nuclei of EPCs were identified by DAPI staining. Scale bars: 10 μm (a and b); 2 μm (d and e); 5 μm (f and g).

GFP-expressing EPCs were incorporated into the walls of pulmonary arterioles in MCT rats and composed pulmonary vasculature (Figure 4a). Transplanted GFP-expressing EPCs were distributed on lung tissues (Figure 4b). AM gene-transduced EPCs were similarly incorporated into the pulmonary vasculature (Figure 4c). Immunohistochemical analyses of rat and human CD31 demonstrated that the transplanted EPCs were of endothelial lineage and comprised a vessel structure similar to rat endothelial cells (Figure 4c). However, transplanted EPCs were rarely distributed to other tissues such as cardiac ventricles, kidneys, aorta, and brain (data not shown).

Effects of Gene-Transduced EPC Transplantation on Pulmonary Hypertension

Pulmonary hypertension developed 3 weeks after MCT injection. Mean pulmonary arterial pressure was not strikingly decreased in the EPC group (−14%) but was significantly lower in the AM-EPC group (−29%) than in the control group (Figure 5a). Pulmonary vascular resistance was significantly lower in both the EPC group (−16%) and the AM-EPC group (−39%) than in the control group (Figure 5b). Importantly, the AM-EPC group showed significantly greater improvement in pulmonary vascular resistance than the EPC group. Right ventricular weight and right ventricular

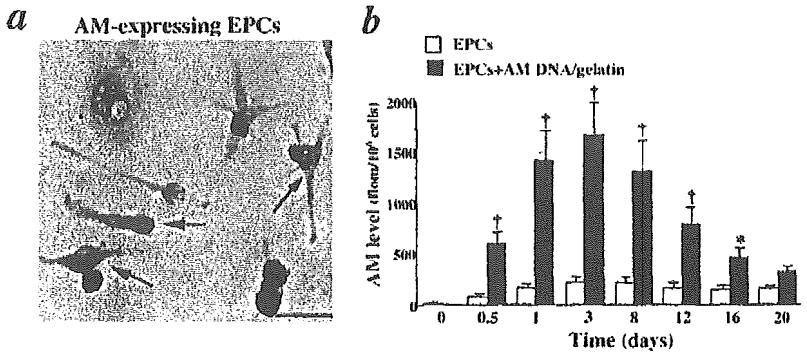

Figure 3. AM gene transfer into EPCs. a, Immunohistochemical analysis of AM in EPCs after gene transfer. Intense immunostaining for AM was observed in EPCs (arrows). Scale bar: 10 μm. b, Time course of AM secretion from EPCs during coculture with AM DNA-gelatin complexes. Data are mean±SEM. *$P<0.05$, †$P<0.001$ vs EPCs.

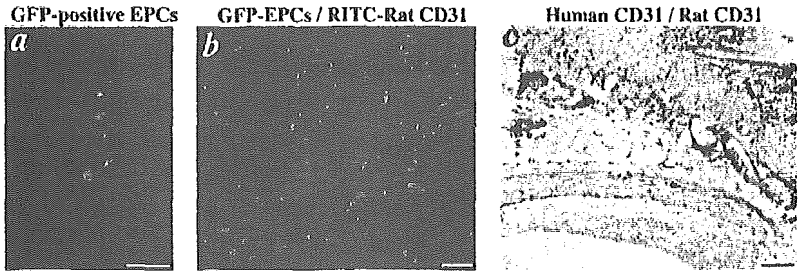

Figure 4. Distribution of EPCs in lungs of MCT rats. a, Intravenously administered GFP-expressing EPCs were incorporated into walls of pulmonary arterioles. b, Transplanted GFP-expressing EPCs were distributed on lung tissues. Pulmonary vasculature was detected by RITC-conjugated anti-rat CD31 (red). c, Immunohistochemistry for human CD31 (peroxidase, brown) and rat CD31 (alkaline phosphatase, pink). Scale bars: 50 μm.

systolic pressure were significantly lower in the AM-EPC group than in the control and EPC groups (Table). AM levels in plasma and lung tissues were significantly higher in the AM-EPC group than in the other groups 2 weeks after transplantation. Unlike EPCs, transplantation of mature pulmonary artery endothelial cells did not significantly influence pulmonary hemodynamics in MCT rats.

Representative photomicrographs showed that hypertrophy of the pulmonary vessel wall after MCT injection was attenuated in both the EPC and AM-EPC groups (Figure 5c). Quantitative analysis also demonstrated a significant increase in percent wall thickness after MCT injection, but this change was markedly attenuated in the AM-EPC group (Figure 5d). Kaplan-Meier survival curves demonstrated that MCT rats transplanted with AM-expressing EPCs (AM-EPC group) had a significantly higher survival rate than those given culture medium (control group) or EPCs alone (EPC group; Figure 5e).

Discussion

In the present study, we present a new concept for cell-based gene delivery into the pulmonary vasculature that consists of 3 processes. First, cationic gelatin is readily complexed with plasmid DNA. Second, EPCs phagocytose ionically linked plasmid DNA-gelatin complexes in coculture, which allows nonviral gene transfer into EPCs with high efficiency. Third, transplanted gene-modified EPCs are incorporated into pulmonary vascular beds in MCT rats. This novel gene delivery system has great advantages over conventional gene therapy: nonviral, noninvasive, and highly efficient gene targeting into the pulmonary vasculature. These benefits may be achieved mainly by the ability of EPCs to phagocytose DNA-gelatin complexes and to migrate to sites of injured endothelium.

Tabata et al[7] and Fukunaka et al[8] demonstrated that gelatin can hold negatively charged protein or plasmid DNA in its positively charged lattice structure. In addition, Tabata et al[9] demonstrated that gelatin is promptly phagocytosed and gradually degraded by macrophages. The present study first demonstrated that EPCs phagocytosed ionically linked DNA-gelatin complexes, dissolved gelatin, and freed the DNA. Surprisingly, the transfection efficiency of this approach was markedly high. FACS analysis demonstrated that EPCs, not monocytes/macrophages, are the main contributors of GFP expression. These findings suggest that the phagocytosing action of EPCs allows nonviral, highly efficient gene transfer into EPCs themselves.

Recently, intravenously administered hematopoietic cells have been shown to be attracted to sites of cerebral injury.[18] Intravenously injected EPCs accumulate in ischemic myocar-

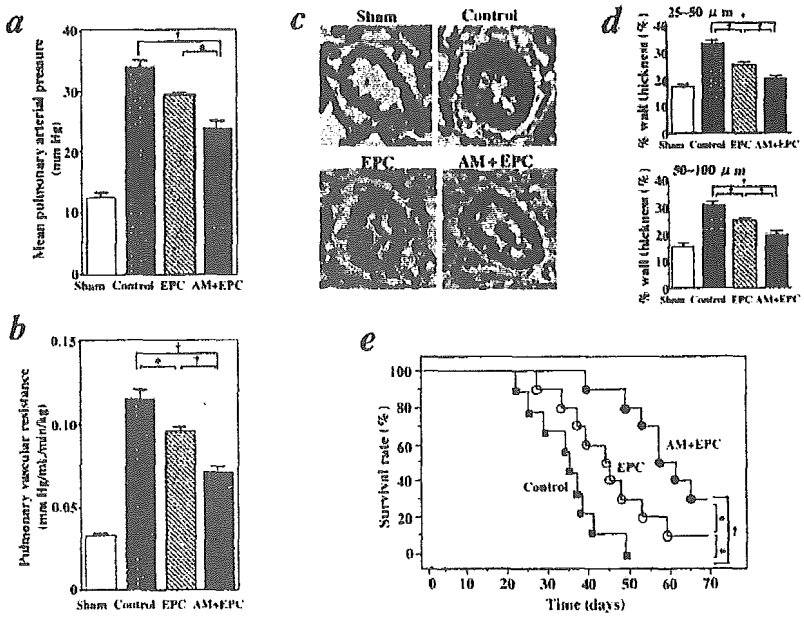

Figure 5. Effects of AM DNA-transduced EPC transplantation on mean pulmonary arterial pressure (a) and pulmonary vascular resistance (b) in MCT rats. c, Representative photomicrographs of peripheral pulmonary arteries in rats. Scale bars, 20 μm. d, Quantitative analysis of percent wall thickness of peripheral pulmonary arteries. e, Kaplan-Meier survival curves of MCT rats transplanted with AM-expressing EPCs (AM-EPC group, ●), EPCs alone (EPC group, ○), or culture medium (control group, □). Data are mean±SEM. *$P<0.05$; †$P<0.001$.

Physiological Profiles of 4 Experimental Groups

	Sham (n=8)	Control (n=9)	EPC (n=8)	AM-EPC (n=9)
Body weight, g	191±4	174±7	181±6	182±6
RV weight, g/kg body weight	0.59±0.02	1.04±0.05	0.91±0.03	0.77±0.04*†
Left ventricular weight, g/kg body weight	2.42±0.03	2.49±0.05	2.46±0.04	2.44±0.09
Heart rate, bpm	398±10	390±11	398±15	387±11
Mean arterial pressure, mm Hg	112±4	100±5	104±3	98±4
RV systolic pressure, mm Hg	32±2	63±3	56±1*	48±2*†
Plasma human AM, fmol/mL	0	0	0.3±0.1*	0.7±0.1*†
Lung human AM, fmol/g tissue	0	0	11.9±0.6*	23.0±2.3*†

Control indicates MCT rats given culture medium; EPC, MCT rats given EPCs; AM-EPC, MCT rats given AM-expressing EPCs; and RV, right ventricular. Data are mean±SEM.

*$P<0.05$ vs control; †$P<0.05$ vs EPC.

dium after acute myocardial infarction.[6] These findings suggest that progenitor cells have the ability to sense injured tissues. In fact, in the present study, intravenously administered GFP-expressing EPCs were incorporated into pulmonary arterioles and capillaries in MCT rats and differentiated mature endothelial cells. MCT injures endothelial cells of small arteries and capillaries in the lungs, resulting in pulmonary hypertension.[19] Taking these findings together, transplanted EPCs may circulate in the blood and attach to injured pulmonary endothelia in MCT rats. Thus, EPCs may serve not only as a vehicle for gene delivery to injured pulmonary endothelia but also as a tissue-engineering tool in restoring intact pulmonary endothelium. Transplantation of EPCs without gene modification slightly but significantly decreased pulmonary vascular resistance in MCT rats. EPCs have been shown to express endothelial nitric oxide synthase and produce nitric oxide.[14] In the present study, we showed that EPCs produce AM even when its gene is not transduced. These results suggest that vasodilator substances secreted from EPCs contribute to improvement in pulmonary hypertension.

We also investigated whether transplantation of gene-modified EPCs causes additional improvement in pulmonary hemodynamics and survival in MCT rats. AM is one of the most potent vasodilators synthesized by vascular endothelial cells.[1] Interestingly, EPCs cultured with AM DNA-gelatin complexes markedly secreted AM protein for more than 16 days. These results suggest relatively long-lasting AM secretion from EPCs. The consequence of this synthesis in MCT rats was a marked decrease in mean pulmonary arterial pressure and pulmonary vascular resistance. Histological examination revealed that transplantation of AM-expressing EPCs inhibited an increase in medial wall thickness of pulmonary arteries. Expectedly, transplantation of AM-expressing EPCs caused significantly greater improvement in pulmonary hypertension and vascular remodeling than transplantation of EPCs alone. Given the known potent vasoprotective effects of AM, such as vasodilation and inhibition of smooth muscle cell proliferation,[1,20] it is interesting to speculate that AM secreted from EPCs may act not only as a circulating factor but also as an autocrine/paracrine factor in the regulation of pulmonary vascular tone and vascular remodeling in MCT rats. Importantly, a single transplantation of AM-expressed EPCs improved survival in MCT rats compared with administration of EPCs alone or culture medium. These results suggest that ex vivo gene transfer into EPCs greatly enhances the therapeutic effects of EPC transplantation. Additional studies are necessary to examine whether repeated administration of EPCs produces an even greater effect than single transplantation.

Conclusions

Human umbilical cord blood–derived EPCs have a phagocytosing action that allows nonviral, highly efficient gene transfer into EPCs. Transplantation of AM DNA-transduced EPCs causes significantly greater improvement in pulmonary hypertension and better survival in MCT rats than transplantation of EPCs alone. Thus, the novel hybrid cell–gene therapy based on the phagocytosing action of EPCs may be a new therapeutic strategy for the treatment of pulmonary hypertension.

Acknowledgments

This work was supported by a grant from the Japan Cardiovascular Research Foundation; HLSRG-RAMT-nano-001 and -RHGTEFB-genome-005, RGCD13C-1 from the Ministry of Health, Labour, and Welfare (MHLW); grants from NEDO; a grant-in-aid for scientific research from the Ministry of Education, Culture, Sports, Science, and Technology (13470154 and 13877114); the Promotion of Fundamental Studies in Health Science of the Organization for Pharmaceutical Safety and Research (OPSR) of Japan; and a grant for Research on Human Genome, Tissue Engineering Food Biotechnology, application of cord blood for blood transplantation and tissue engineering from MHLW. We thank Dr Atsuhiko Kawamoto for his technical assistance.

References

1. Kitamura K, Kangawa K, Kawamoto M, et al. Adrenomedullin: a novel hypotensive peptide isolated from human pheochromocytoma. *Biochem Biophys Res Commun.* 1993;192:553–560.
2. Archer S, Rich S. Primary pulmonary hypertension: a vascular biology and translational research "work in progress." *Circulation.* 2000;102:2781–2791.
3. Asahara T, Murohara T, Sullivan A, et al. Bone marrow origin of endothelial progenitor cells responsible for postnatal vasculogenesis in physiological and pathological neovascularization. *Science.* 1997;275:965–967.

4. Takahashi T, Kalka C, Masuda H, et al. Ischemia- and cytokine-induced mobilization of bone marrow-derived endothelial progenitor cells for neovascularization. *Nat Med.* 1999;5:434–438.
5. Gill M, Dias S, Hattori K, et al. Vascular trauma induces rapid but transient mobilization of VEGFR2(+)AC133(+) endothelial precursor cells. *Circ Res.* 2001;88:167–174.
6. Kawamoto A, Gwon HC, Iwaguro H, et al. Therapeutic potential of ex vivo expanded endothelial progenitor cells for myocardial ischemia. *Circulation.* 2001;103:634–637.
7. Tabata Y, Nagano A, Ikada Y. Biodegradation of hydrogel carrier incorporating fibroblast growth factor. *Tissue Eng.* 1999;5:127–138.
8. Fukunaka Y, Iwanaga K, Morimoto K, et al. Controlled release of plasmid DNA from cationized gelatin hydrogels based on hydrogel degradation. *J Control Release.* 2002;80:333–343.
9. Tabata Y, Ikada Y. Macrophage activation through phagocytosis of muramyl dipeptide encapsulated in gelatin microspheres. *J Pharm Pharmacol.* 1987;39:698–704.
10. Owji AA, Smith DM, Coppock HA, et al. An abundant and specific binding site for the novel vasodilator adrenomedullin in the rat. *Endocrinology.* 1995;136:2127–2134.
11. Yoshibayashi M, Kamiya T, Kitamura K, et al. Plasma levels of adrenomedullin in primary and secondary pulmonary hypertension in patients <20 years of age. *Am J Cardiol.* 1997;79:1556–1558.
12. Nagaya N, Satoh T, Nishikimi T, et al. Hemodynamic, renal and hormonal effects of adrenomedullin infusion in patients with congestive heart failure. *Circulation.* 2000;101:498–503.
13. Nagaya N, Nishikimi T, Uematsu M, et al. Haemodynamic and hormonal effects of adrenomedullin in patients with pulmonary hypertension. *Heart.* 2000;84:653–658.
14. Murohara T, Ikeda H, Duan J, et al. Transplanted cord blood-derived endothelial precursor cells augment postnatal neovascularization. *J Clin Invest.* 2000;105:1527–1536.
15. Kalka C, Masuda H, Takahashi T, et al. Vascular endothelial growth factor (165) gene transfer augments circulating endothelial progenitor cells in human subjects. *Circ Res.* 2000;86:1198–1202.
16. Dimmeler S, Aicher A, Vasa M, et al. HMG-CoA reductase inhibitors (statins) increase endothelial progenitor cells via the PI 3-kinase/Akt pathway. *J Clin Invest.* 2001;108:391–397.
17. Kalka C, Masuda H, Takahashi T, et al. Transplantation of ex vivo expanded endothelial progenitor cells for therapeutic neovascularization. *Proc Natl Acad Sci U S A.* 2000;97:3422–3427.
18. Priller J, Flugel A, Wehner T, et al. Targeting gene-modified hematopoietic cells to the central nervous system: use of green fluorescent protein uncovers microglial engraftment. *Nat Med.* 2001;7:1356–1361.
19. Rosenberg H, Rabinovitch M. Endothelial injury and vascular reactivity in monocrotaline pulmonary hypertension. *Am J Physiol.* 1988;255:H1484–H1491.
20. Horio T, Kohno M, Kano H, et al. Adrenomedullin as a novel antimigration factor of vascular smooth muscle cells. *Circ Res.* 1995;77:660–664.

Adrenomedullin Gene Transfer Induces Therapeutic Angiogenesis in a Rabbit Model of Chronic Hind Limb Ischemia

Benefits of a Novel Nonviral Vector, Gelatin

Noriyuki Tokunaga, MD; Noritoshi Nagaya, MD; Mikiyasu Shirai, MD; Etsuro Tanaka, MD; Hatsue Ishibashi-Ueda, MD; Mariko Harada-Shiba, MD; Munetake Kanda, MD; Takefumi Ito, MD; Wataru Shimizu, MD; Yasuhiko Tabata, PhD; Masaaki Uematsu, MD; Kazuhiro Nishigami, MD; Shunji Sano, MD; Kenji Kangawa, PhD; Hidezo Mori, MD

Background—Earlier studies have shown that adrenomedullin (AM), a potent vasodilator peptide, has a variety of cardiovascular effects. However, whether AM has angiogenic potential remains unknown. This study investigated whether AM gene transfer induces therapeutic angiogenesis in chronic hind limb ischemia.

Methods and Results—Ischemia was induced in the hind limb of 21 Japanese White rabbits. Positively charged biodegradable gelatin was used to produce ionically linked DNA-gelatin complexes that could delay DNA degradation. Human AM DNA (naked AM group), AM DNA-gelatin complex (AM-gelatin group), or gelatin alone (control group) was injected into the ischemic thigh muscles. Four weeks after gene transfer, significant improvements in collateral formation and hind limb perfusion were observed in the naked AM group and AM-gelatin group compared with the control group (calf blood pressure ratio: 0.60±0.02, 0.72±0.03, 0.42±0.06, respectively). Interestingly, hind limb perfusion and capillary density of ischemic muscles were highest in the AM-gelatin group, which revealed the highest content of AM in the muscles among the three groups. As a result, necrosis of lower hind limb and thigh muscles was minimal in the AM-gelatin group.

Conclusions—AM gene transfer induced therapeutic angiogenesis in a rabbit model of chronic hind limb ischemia. Furthermore, the use of biodegradable gelatin as a nonviral vector augmented AM expression and thereby enhanced the therapeutic effects of AM gene transfer. Thus, gelatin-mediated AM gene transfer may be a new therapeutic strategy for the treatment of peripheral vascular diseases. (***Circulation***. **2004;109:526-531.**)

Key Words: peripheral vascular disease ■ angiogenesis ■ gene therapy ■ ischemia

Adrenomedullin (AM) is a potent vasodilator peptide that was originally isolated from human pheochromocytoma.[1] AM and its receptor are expressed mainly in vascular endothelial cells and vascular smooth muscle cells.[2–4] AM not only induces vasorelaxation but also regulates growth and death of these vascular cells.[5–10] These findings suggest that AM plays an important role in maintaining vascular homeostasis in an autocrine and/or paracrine manner.

A recent study has shown that vascular abnormalities are present in homozygous AM knockout mice, suggesting that AM is indispensable for vascular morphogenesis.[11–13] More recently, AM has been shown to activate the PI3K/Akt-dependent pathway in vascular endothelial cells, which is considered to regulate multiple critical steps in angiogenesis, including endothelial cell survival, proliferation, migration, and capillary-like structure formation.[7,14] These results raise the possibility that AM plays a role in modulating vasculogenesis and angiogenesis. However, whether AM induces therapeutic angiogenesis remains unknown.

Received May 20, 2003; revision received September 25, 2003; accepted September 26, 2003.

From the Department of Cardiac Physiology, National Cardiovascular Center Research Institute, Osaka, Japan (N.T., M.S., M.K., H.M.); the Department of Cardiovascular Surgery, Okayama University Medical School, Okayama, Japan (N.T., S.S.); the Department of Regenerative Medicine and Tissue Engineering, National Cardiovascular Center Research Institute, Osaka, Japan (N.N., T.I.); the Department of Internal Medicine, National Cardiovascular Center, Osaka, Japan (N.N., W.S., K.N.); the Department of Physiology, the Research Center for Genetic Engineering and Cell Transplantation, Tokai University School of Medicine, Isehara, Japan (E.T.); the Department of Pathology, National Cardiovascular Center, Osaka, Japan (H.I.-U.); the Department of Biochemistry, National Cardiovascular Center Research Institute, Osaka, Japan (M.H.-S., K.K.); the Department of Biomaterials, Field of Tissue Engineering, Institute for Frontier Medical Sciences, Kyoto University, Kyoto, Japan (Y.T.); and the Cardiovascular Division, Kansai Rosai Hospital, Hyogo, Japan (M.U.).

Correspondence to Noritoshi Nagaya, MD, Department of Regenerative Medicine and Tissue Engineering or Hidezo Mori, MD, Department of Cardiac Physiology, National Cardiovascular Center Research Institute, 5-7-1 Fujishirodai, Suita, Osaka 565-8565, Japan. E-mail nagayann@hsp.ncvc.go.jp or hidemori@ri.ncvc.go.jp

Circulation is available at http://www.circulationaha.org

DOI: 10.1161/01.CIR.0000109700.81266.32

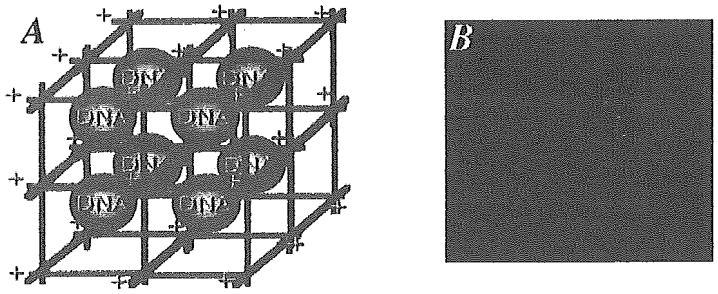

Figure 1. A, Schema of DNA-gelatin complex. Biodegradable gelatin can hold negatively charged plasmid DNA in its positively charged lattice structure. B, RITC-labeled AM DNA particles were incorporated into gelatin.

We prepared biodegradable gelatin that could hold negatively charged protein or plasmid DNA in its positively charged lattice structure.[15,16] Biodegradable gelatin has been widely used as a carrier of protein because of its capacity to delay protein degradation.[15] Similarly, ionically linked DNA-gelatin complexes can delay gene degradation.[16] These findings raise the possibility that gelatin may serve as a nonviral vector for gene therapy.

Thus, the purposes of this study were (1) to investigate whether AM gene transfer induces therapeutic angiogenesis in a rabbit model of chronic hind limb ischemia and (2) to examine whether the use of biodegradable gelatin as a vector augments AM expression and thereby enhances the therapeutic effects of AM gene transfer.

Methods

Animal Model

All protocols were performed in accordance with the guidelines of the Animal Care Ethics Committee of the National Cardiovascular Center Research Institute. Twenty-one male Japanese White rabbits (body weight, 2.9±0.1 kg; Japan Animal Co, Osaka, Japan) were used for physiological and morphological assessment. In addition, 30 rabbits were used for radioimmunoassay, immunohistochemical examination, and Western blot analysis. After anesthetization with pentobarbital sodium (30 to 35 mg/kg), a longitudinal incision was made in the left thigh, extending inferiorly from the inguinal ligament to a point just proximal to the patella. Hind limb ischemia was induced by ligation of the distal left external iliac artery and complete resection of the left femoral artery, as described previously.[17]

Construction of Plasmid DNA

To construct the expression vector for human AM, the *EcoRI/XhoI* fragment of the full-length human AM cDNA was ligated into the EcoRI/XhoI fragment of the pcDNA1.1-CMV expression plasmid (Invitrogen). To verify that the pcDNA1.1-CMV vector encoding AM cDNA produces a biologically active AM protein, the expression vector was transfected into 293 cells, and AM activity in the transfected cells was measured by high-performance liquid chromatography and radioimmunoassay. The pcDNA1.1-CMV vector encoding β-galactosidase (LacZ) cDNA was used as a control DNA.

Preparation of AM DNA-Gelatin Complex

Biodegradable gelatin was prepared from pig skin. The gelatin was characterized by a spheroid shape with a diameter of approximately 30 μm, water content of 95%, and an isoelectric point (pI) of 9 after swelling in water.[15,16] Gelatin can hold negatively charged protein or plasmid DNA in its positively charged lattice structure (Figure 1A). Dried gelatin (4 mg, pI 9) was added to human AM DNA solution (500 μg/100 μL in phosphate-buffered saline, pH 7.4). After mixture of DNA and gelatin, DNA-gelatin complexes were incubated at 37°C for 2 hours.

To visualize incorporation of DNA into gelatin, AM plasmid DNA was labeled with rhodamine B isothiocyanate (RITC), as reported previously.[16] In brief, the coupling reaction of RITC to plasmid DNA was carried out by mixing the two substances in 0.2 mol/L sodium carbonate-buffered solution (pH 9.7), followed by gel filtration with a PD 10 column (Amersham-Pharmacia). RITC-labeled AM DNA was incorporated into positively charged gelatin (Figure 1B).

Study Protocol

Ten days after the induction of hind limb ischemia (day 10), AM DNA (naked AM group, n=7), AM DNA-gelatin complex (AM-gelatin group, n=7), or gelatin alone (control group, n=7) was administered intramuscularly into 3 different sites in the ischemic adductor muscle and 2 different sites in the semimembranous muscle. In addition, Lac Z DNA-gelatin complex served as a control DNA (Lac Z-gelatin group, n=5). The amount of plasmid was 500 μg (1 mL) and that of gelatin was 4 mg. Morphological and angiographic analyses and measurements of calf blood pressure and laser Doppler flow were performed 4 weeks after gene transfer (day 38). After completion of these measurements, the adductor, semimembranous, and gastrocnemius muscles were weighed in each hind limb.[18] The muscle weight ratio was calculated for each muscle as follows: muscle weight ratio=muscle weight in ischemic hind limb/muscle weight in nonischemic hind limb. Specimens of the adductor muscle of the ischemic hind limb were obtained for histological examination.

Measurement of Calf Blood Pressure

Calf blood pressure was measured on days 10 and 38 in both hind limbs with a Doppler flowmeter (Hayashi Denki Co, Ltd) and a 25-mm-wide cuff. The pulse of the posterior tibial artery was identified with the use of a Doppler probe, and the systolic blood pressure in both hind limbs was determined by standard techniques. The calf blood pressure ratio was defined for each rabbit as the ratio of systolic pressure of the ischemic hind limb to that of the normal hind limb.[17]

Laser Doppler Blood Perfusion Analysis

Blood flow of the ischemic hind limb was measured with the use of a laser Doppler blood perfusion image system (moorLDI, Moor Instruments) on day 38.

Angiographic Analysis

Development of collateral arteries was evaluated by angiography on days 0 and 38. A 4F catheter was placed in the left internal iliac artery through the common carotid artery, and 3 mL contrast medium (Iopamiron 300, SCHERING) was injected with an automated angiography injector at a rate of 2.5 mL/s. Quantitative angiographic analysis of collateral vessel development in the ischemic hind limb was performed with the use of a 5-mm^2 grid overlay, as described previously.[17] The angiographic score was calculated for each film as the ratio of grid intersections crossed by opacified arteries divided by the total number of grid intersections in the ischemic medial thigh. The angiographic score was determined by 2 blinded observers.

Morphological and Histological Examination

The degree of lower hind limb necrosis and thigh muscle necrosis was macroscopically evaluated on graded morphological scales (grade 1 to 3) for peripheral tissue damage and muscle necrosis area of the adductor, semimembranous, and medial large muscles. Capillary density of the ischemic hind limb was evaluated by alkaline phosphatase staining, as reported previously.[17] A total of 10 different fields from three different sections were randomly selected, and the number of capillaries was counted under a ×40 objective. Capillary density was expressed as the mean number of capillaries per square millimeter. The number of myofibers in each field was also examined and the capillary/muscle fiber ratio calculated.

Radioimmunoassay for Human AM

Human AM production was examined 1, 2, and 4 weeks after gene transfer in the naked AM group, AM-gelatin group, and control group (n=5 each). The muscles were harvested for radioimmunoassay and immunohistochemical examination. Immunoreactive human AM level in rabbit muscles was determined by immunoradiometric assay with the use of a specific kit (Shionogi Co, Ltd).[19] Tissue content of vascular endothelial growth factor (VEGF) was examined by ELISA kit (R&D systems).

Immunohistochemistry for Human AM, Ki67 Antigen, and Phosphorylated Akt

Immunohistochemical studies were performed on formalin-fixed, paraffin-embedded 4-μm sections of ischemic thigh muscles 7 days after gene transfer. To elucidate AM expression after gene therapy, immunohistochemistry for human AM was performed with the use of a monoclonal antibody recognizing AM-(12–25) (1:100), as reported previously.[20] To evaluate the proliferative potential of AM, tissue sections were stained for Ki67, a marker for cell proliferation, with the use of monoclonal anti-Ki67 antibody (1:100) (DAKO). AM has recently been shown to promote proliferation of vascular endothelial cells at least in part through the PI3k/Akt pathway.[21] Thus, immunohistochemistry for phosphorylated Akt was performed with mouse monoclonal anti-phosphorylated Akt antibody (1:100) (Cell Signaling Technology).

Western Blot Analysis

To identify Akt phosphorylation in ischemic muscles after AM gene transfer, Western blotting was performed with the use of a commercially available kit (PhosphoPlus Akt [Ser473] Antibody Kit, Cell Signaling Technology). Ischemic muscles in the 3 groups were obtained 7 days after AM gene transfer. These samples were homogenized on ice in 0.1% Tween 20 homogenization buffer with a protease inhibitor (Complete, Roche). After centrifugation for 20 minutes at 4°C, the supernatant was used for Western blot analysis. The 50 μg of protein was transferred into sample buffer, loaded on 7.5% SDS-polyacrylamide gel, and blotted onto nitrocellulose membrane through the use of a wet blotting system. After blocking for 60 minutes, the membranes were incubated with primary antibodies (1:500) at 4°C overnight. The membranes were then incubated with secondary antibodies, which were conjugated with horseradish peroxidase (Cell Signaling Technology), at a final dilution of 1:2000. Signals were detected through the use of LumiGLO chemiluminescence reagents (Cell Signaling Technology).

Statistical Analysis

All results are expressed as mean±SEM. Statistical significance was evaluated by 1-way ANOVA followed by Fisher's analysis, Scheffe's F analysis, or Kruskal-Wallis test. A value of $P<0.05$ was considered statistically significant.

Results

Physiological and Morphological Assessment

Complete resection of the left femoral artery resulted in a similar decrease in calf blood pressure ratio among the 3 groups before the initiation of therapy (day 10) (Figure 2A). However, the calf blood pressure ratio on day 38 was highest in the AM-gelatin groups, followed by the naked AM group and subsequently the control group. The laser Doppler flow in hind limb was highest in the AM-gelatin group, followed by the naked AM group and the control group (Figure 2B). The calf blood pressure ratio and laser Doppler flow 4 weeks after gene transfer did not significantly differ between the control group and Lac Z-gelatin group. Lower hind limb necrosis was minimal in the AM-gelatin group, followed by the naked AM group and the control group (Figure 2C). Thigh muscle necrosis was also minimal in the AM-gelatin group. Similarly, the muscle weight ratio (ischemic/normal) on day 38 was highest in the AM-gelatin group (Table). Neither mean arterial pressure nor heart rate significantly differed among the 3 groups.

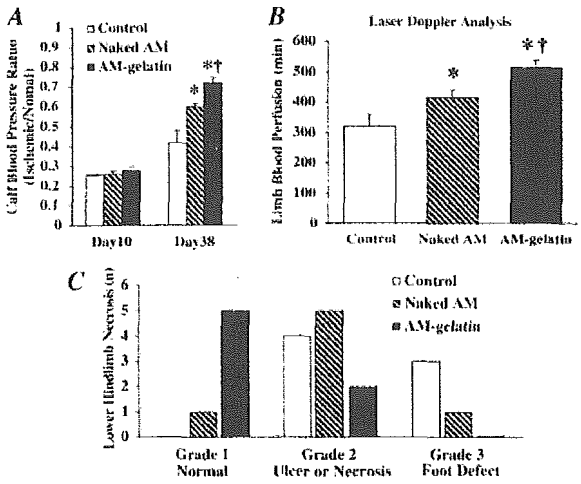

Figure 2. A, Calf blood pressure ratio (ischemic/normal hind limb) before (on day 10) and after (on day 38) gene transfer. B, Measurement of laser Doppler flow on day 38. Data are mean±SEM. *$P<0.05$ vs control group; †$P<0.05$ vs naked AM group. C, Number of cases of each grade of lower hind limb necrosis on day 38. Lower hind limb necrosis was minimal in the AM-gelatin group. Number of necrosis or foot defect is statistically significant among the 3 groups ($P<0.05$ by Kruskal-Wallis test).

Angiographic Analysis

Angiograms 4 weeks after gene transfer (day 38) showed the development of collateral arteries in the naked AM and

Physiological Characteristics

	Control	Naked AM	AM-Gelatin
No. of rabbits	7	7	7
Body weight, kg	2.46±0.06	2.65±0.10	3.16±0.09
MAP, mm Hg	112±3	114±3	116±2
HR, beats/min	269±12	253±5	262±7
Muscle weight ratio	0.71±0.03	0.84±0.02*	0.95±0.02*†

MAP indicates mean arterial pressure; HR, heart rate; and muscle weight ratio, ratio of muscle weight in ischemic hind limb to that in nonischemic hind limb. Data are mean±SEM.

*$P<0.01$ vs control group; †$P<0.05$ vs naked AM group.

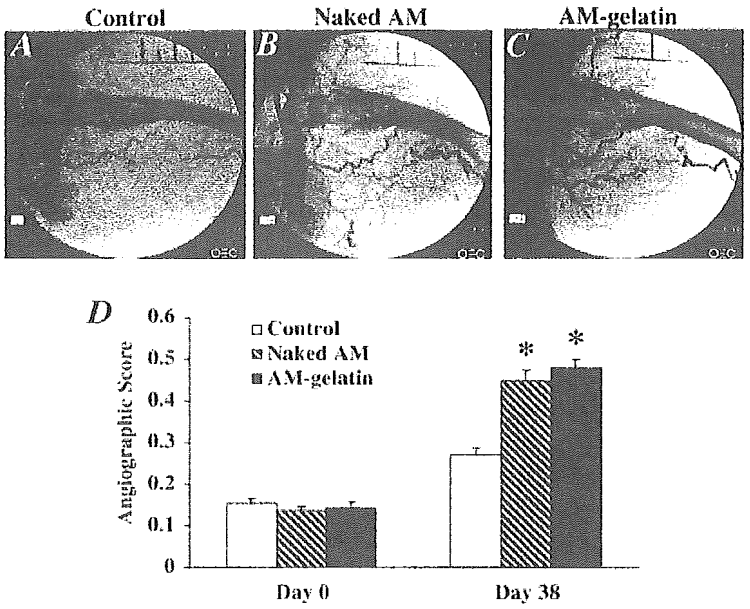

Figure 3. Representative angiograms of control group (A), naked AM group (B), and AM-gelatin group (C) on day 38. Collateral arteries were well developed in the naked AM and AM-gelatin groups. D, Angiographic score on days 0 and 38 in each group. Angiographic score on day 38 was significantly higher in the naked AM and AM-gelatin groups than in the control group. Data are mean±SEM. *$P<0.001$ versus control group.

AM-gelatin groups compared with that in the control group (Figure 3, A through C). Quantitative analysis of collateral vessels demonstrated that the angiographic score in both the naked AM and AM-gelatin groups was significantly higher than that in the control group (Figure 3D). Angiographic score did not significantly differ between the control group and Lac Z-gelatin group.

To examine the development of collateral vessels in an earlier stage, other rabbits (n=4 each) were examined 2 weeks after gene transfer (day 24). Angiograms showed significant collateral development in the naked AM and AM-gelatin groups compared with that in the control group.

Histological Examination

Alkaline phosphatase staining of ischemic hind limb muscle showed marked augmentation of neovascularization in both the naked AM and AM-gelatin groups compared with the control group (Figure 4, A through C). Quantitative analysis demonstrated that capillary density of the ischemic adductor muscle was highest in the AM-gelatin group (Figure 4D). Analysis of the capillary/muscle fiber ratio yielded similar results. Seven days after gene transfer, intense immunostaining for Ki67 was observed in vascular endothelial cells of the naked AM and the AM-gelatin groups (Figure 4, E through G).

AM Expression and Akt Phosphorylation After Gene Transfer

Seven days after gene transfer, modest immunostaining for human AM was observed in the naked AM group, whereas AM immunoreactivity was intense surrounding the gelatin in the AM-gelatin group (Figure 5, A through C). Tissue content of human AM was significantly increased both in the naked AM and the AM-gelatin groups 7 days after gene transfer (Figure 5D). The AM level in the AM-gelatin group was significantly higher that in the naked AM group. Two weeks after gene transfer, AM overexpression was observed only in the AM-gelatin group. The expression of endogenous VEGF and its receptors (Flt-1 and Flk-1) did not differ among the 3 groups (data not shown). Western blot analysis revealed that phosphorylated Akt in ischemic muscles was increased in both the naked AM and AM-gelatin groups 7 days after gene transfer (Figure 5E). Intense immunostaining for phosphory-

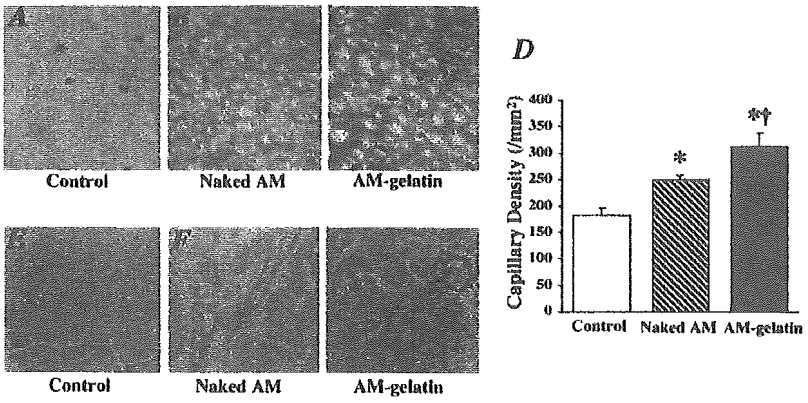

Figure 4. A through C, Representative examples of alkaline phosphatase staining in ischemic hind limb muscles. Magnification ×200. D, Quantitative analysis of capillary density in ischemic hind limb muscles. Data are mean±SEM. *$P<0.05$ vs control group; †$P<0.05$ vs naked AM group. E through G, Immunohistochemical analysis of Ki67 antigen, a marker for cell proliferation. Magnification ×400.

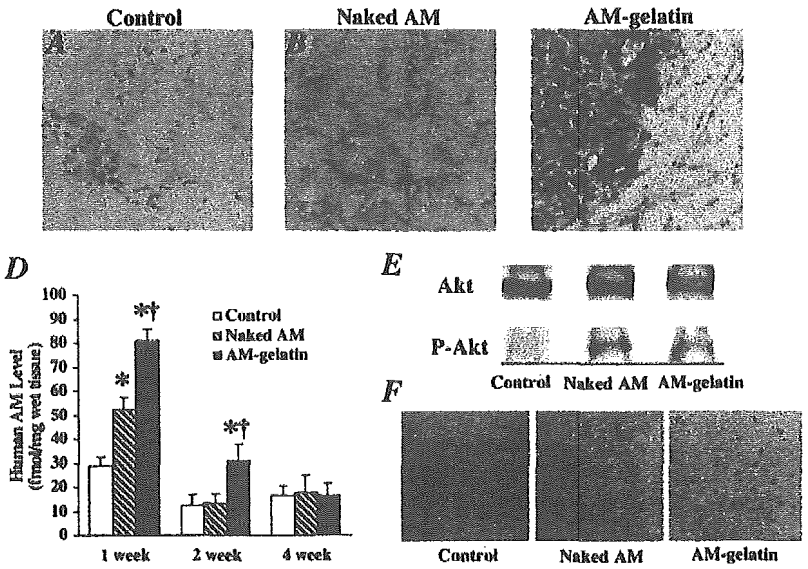

Figure 5. A through C, Immunohistochemistry for human AM 7 days after gene transfer. Intense immunostaining was observed surrounding gelatin in the AM-gelatin group. Magnification ×200. D, Time course of AM production in ischemic muscles after gene transfer. Data are mean±SEM. *$P<0.01$ vs control group; †$P<0.01$ vs naked AM group. E, Western blot analysis for Akt phosphorylation in muscles. F, Immunohistochemical staining for phosphorylated Akt 7 days after gene transfer. Phosphorylated Akt was distributed at least in endothelial cells. Magnification ×400.

lated Akt was observed at least in endothelial cells of the Naked AM and the AM-gelatin groups (Figure 5F).

Discussion

We demonstrated that (1) AM gene transfer induced hemodynamic and angiographic improvements in association with an increase in capillary density in a rabbit model of chronic hind limb ischemia. We also demonstrated that (2) administration of AM DNA-gelatin complexes markedly augmented AM expression and thereby enhanced the therapeutic effects of AM gene transfer.

AM has a variety of effects on the vasculature that include vasodilation,[1,5–7] inhibition of endothelial cell apoptosis,[8,9] and regulation of smooth muscle cell proliferation.[10] However, whether AM has angiogenic potential has remained unknown. In the present study, intramuscular administration of naked AM DNA augmented AM production in skeletal muscles, as indicated by increased tissue content and significant immunostaining of AM. As a result, AM gene transfer increased hind limb perfusion and ameliorated lower hind limb and thigh muscle necrosis in a rabbit model of hind limb ischemia. AM gene transfer may protect the ischemic hind limb partly by improving the blood flow in the ischemic hind limb because AM is originally identified as a potent vasodilating peptide.[1] Nevertheless, angiographic collateral development and high capillary density were observed in ischemic muscles after AM gene transfer. Ki67, a marker for cell proliferation, was detected in endothelial cells of microvessels after AM gene transfer. These results suggest that AM overproduction resulting from gene transfer may induce angiogenesis in a rabbit model of hind limb ischemia. Recent studies using AM gene knockout mice have shown that AM is essential for development of the vasculature during embryogenesis.[11–13] These studies support our results that AM may be an angiogenic factor. VEGF is known to induce angiogenesis and to regulate endothelial cell survival through the phosphatidylinositol 3-kinase (PI3K)/Akt pathway.[22] Thus, the PI3K/Akt pathway is considered to regulate multiple critical steps in angiogenesis, including endothelial cell survival, proliferation, migration, and capillary-like structure formation.[14] A recent study has reported that AM promotes proliferation and migration of human umbilical vein endothelial cells at least in part through the PI3K/Akt pathway.[21] The present study demonstrated that phosphorylated Akt is increased at least in endothelial cells after AM gene transfer. AM gene transfer did not influence endogenous VEGF and its receptors. Taken together, it is interesting to speculate that AM may directly induce angiogenesis through the PI3K/Akt pathway.

In the present study, we used positively charged biodegradable gelatin as a nonviral vector. We have shown that basic fibroblast growth factor (bFGF) is ionically linked with gelatin, which enhances the angiogenic effects of bFGF by delaying protein degradation.[15] Thus, biodegradable gelatin has been used as a carrier of protein. However, little information is available regarding the therapeutic potential of gelatin as a nonviral vector for gene transfer. In the present study, we demonstrated that RITC-labeled AM DNA was incorporated into positively charged gelatin. In addition, intramuscular administration of AM DNA-gelatin complexes strongly enhanced AM production compared with that of naked AM DNA. These results suggest that biodegradable gelatin may serve as a vector for gene transfer. In fact, AM DNA-gelatin complexes induced more potent angiogenic effects in a rabbit model of hind limb ischemia than naked AM DNA, as evidenced by significant increases in histological capillary density, calf blood pressure ratio, laser Doppler flow, and muscle weight ratio and a decrease in necrosis of lower hind limb and thigh muscles. These results suggest that the use of biodegradable gelatin as a nonviral vector augments AM expression and enhances AM-induced angiogenic effects. The angiogenic effects of AM-gelatin complexes were comparable to those of bFGF-gelatin complexes (data not shown). AM DNA-gelatin complexes were distributed mainly in connective tissues. We have recently demonstrated that gelatin-DNA complex is readily phagocytosed by mac-

rophages, monocytes, endothelial progenitor cells, and so on, resulting in gene expression within these phagocytes.[23,24] These findings raise the possibility that AM secreted from these cells acts on muscles in a paracrine fashion. Unlike AM production in the naked AM group, AM overexpression in the AM-gelatin group lasted for longer than 2 weeks. Thus, it is interesting to speculate that delaying gene degradation by gelatin may be responsible for the highly efficient gene transfer.

Currently, a highly efficient and safe gene delivery system is needed for gene therapy in humans. The present study demonstrated that the use of gelatin, which is considered to be less biohazardous than viral vectors, enhanced the angiogenic potential of AM DNA. Thus, gelatin-mediated AM gene transfer may be a new therapeutic strategy for the treatment of severe peripheral vascular diseases. However, the initial success of gelatin-mediated AM gene therapy reported here should be confirmed by long-term experiments, and extensive toxicity studies in animals are needed before clinical trials.

Study Limitation

First, histological capillary density, calf blood pressure ratio, and laser Doppler flow were significantly higher in the AM-gelatin group than in the naked AM group. However, the angiographic score did not significantly differ between the two. This discrepancy raises the possibility that conventional angiography may have insufficient resolution to fully visualize the angiogenic microvessels. Second, human AM level was slightly elevated in the control group. This implies that the anti-human AM antibody used in this radioimmunoassay had some cross-reactivity with endogenous rabbit AM. Nevertheless, human AM level in the muscles was highest in the AM-gelatin group within 2 weeks after gene transfer. These results suggest that AM DNA-gelatin complexes induces potent and long-lasting AM production.

Conclusions

Intramuscular administration of AM DNA induced therapeutic angiogenesis in a rabbit model of chronic hind limb ischemia. Furthermore, the use of biodegradable gelatin as a nonviral vector augmented AM expression and thereby enhanced the therapeutic effects of AM gene transfer. Thus, gelatin-mediated AM gene transfer may be a new therapeutic strategy for the treatment of peripheral vascular diseases.

Acknowledgments

This work was supported by a grant from the Japan Cardiovascular Research Foundation, HLSRG-RAMT-nano-001 and -RHGTEFB-genome-005, RGCD13C-1 from MHLW, grants from NEDO, a Grant-in-Aid for Scientific research from MECSST (13470154 and13877114), and the Promotion of Fundamental Studies in Health Science of the Organization for Pharmaceutical Safety and Research (OPSR) of Japan.

References

1. Kitamura K, Kangawa K, Kawamoto M, et al. Adrenomedullin: a novel hypotensive peptide isolated from human pheochromocytoma. *Biochem Biophys Res Commun.* 1993;192:553–560.
2. Sugo S, Minamino N, Kangawa K, et al. Endothelial cells actively synthesize and secrete adrenomedullin. *Biochem Biophys Res Commun.* 1994;201:1160–1166.
3. Sugo S, Minamino N, Shoji H, et al. Production and secretion of adrenomedullin from vascular smooth muscle cells: augmented production by tumor necrosis factor-alpha. *Biochem Biophys Res Commun.* 1994;203:719–726.
4. Kato J, Kitamura K, Kangawa K, et al. Receptors for adrenomedullin in human vascular endothelial cells. *Eur J Pharmacol.* 1995;289:383–385.
5. Shimekake Y, Nagata K, Ohta S, et al. Adrenomedullin stimulates two signal transduction pathways, cAMP accumulation and Ca^{2+} mobilization, in bovine aortic endothelial cells. *J Biol Chem.* 1995;270:4412–4417.
6. Nagaya N, Satoh T, Nishikimi T, et al. Hemodynamic, renal, and hormonal effects of adrenomedullin infusion in patients with congestive heart failure. *Circulation.* 2000;101:498–503.
7. Nishimatsu H, Suzuki E, Nagata D, et al. Adrenomedullin induces endothelium-dependent vasorelaxation via the phosphatidylinositol 3-kinase/Akt-dependent pathway in rat aorta. *Circ Res.* 2001;89:63–70.
8. Kato H, Shichiri M, Marumo F, et al. Adrenomedullin as an autocrine/paracrine apoptosis survival factor for rat endothelial cells. *Endocrinology.* 1997;138:2615–2620.
9. Sata M, Kakoki M, Nagata D, et al. Adrenomedullin and nitric oxide inhibit human endothelial cell apoptosis via a cyclic GMP-independent mechanism. *Hypertension.* 2000;36:83–88.
10. Kano H, Kohno M, Yasunari K, et al. Adrenomedullin as a novel antiproliferative factor of vascular smooth muscle cells. *J Hypertens.* 1996;14:209–213.
11. Shindo T, Kurihara Y, Nishimatsu H, et al. Vascular abnormalities and elevated blood pressure in mice lacking adrenomedullin gene. *Circulation.* 2001;104:1964–1971.
12. Caron KM, Smithies O. Extreme hydrops fetalis and cardiovascular abnormalities in mice lacking a functional adrenomedullin gene. *Proc Natl Acad Sci U S A.* 2001;98:615–619.
13. Imai Y, Shindo T, Maemura K, et al. Evidence for the physiological and pathological roles of adrenomedullin from genetic engineering in mice. *Ann N Y Acad Sci.* 2001;947:26–34.
14. Shiojima I, Walsh K. Role of Akt signaling in vascular homeostasis and angiogenesis. *Circ Res.* 2002;90:1243–1250.
15. Tabata Y, Hijikata S, Muniruzzaman M, et al. Neovascularization effect of biodegradable gelatin microspheres incorporating basic fibroblast growth factor. *J Biomater Sci Polym Ed.* 1999;10:79–94.
16. Fukunaka Y, Iwanaga K, Morimoto K, et al. Controlled release of plasmid DNA from cationized gelatin hydrogels based on hydrogel degradation. *J Control Release.* 2002;80:333–343.
17. Takeshita S, Zheng LP, Brogi E, et al. Therapeutic angiogenesis: a single intraarterial bolus of vascular endothelial growth factor augments revascularization in a rabbit ischemic hindlimb model. *J Clin Invest.* 1994;93:662–670.
18. Van Belle E, Witzenbichler B, Chen D, et al. Potentiated angiogenic effect of scatter factor/hepatocyte growth factor via induction of vascular endothelial growth factor. *Circulation.* 1998;97:381–390.
19. Ohta H, Tsuji T, Asai S, et al. A simple immunoradiometric assay for measuring the entire molecules of adrenomedullin in human plasma. *Clin Chim Acta.* 1999;287:B131–B143.
20. Nagaya N, Nishikimi T, Yoshihara F, et al. Cardiac adrenomedullin gene expression and peptide accumulation after acute myocardial infarction in rats. *Am J Physiol Regul Integr Comp Physiol.* 2000;278:R1019–R1026.
21. Miyashita K, Itoh H, Sawada N, et al. Adrenomedullin promotes proliferation and migration of cultured endothelial cells. *Hypertens Res.* 2003;26:S93–S98.
22. Jiang BH, Zheng JZ, Aoki M, et al. Phosphatidylinositol 3-kinase signaling mediates angiogenesis and expression of vascular endothelial growth factor in endothelial cells. *Proc Natl Acad Sci U S A.* 2000;97:1749–1753.
23. Tabata Y, Ikada Y. Macrophage activation through phagocytosis of muramyl dipeptide encapsulated in gelatin microspheres. *J Pharm Pharmacol.* 1987;39:698–704.
24. Nagaya N, Kangawa K, Kanda M, et al. Hybrid cell-gene therapy for pulmonary hypertension based on phagocytosing action of endothelial progenitor cells. *Circulation.* 2003;108:889–895.

Disruption of Autosomal Recessive Hypercholesterolemia Gene Shows Different Phenotype In Vitro and In Vivo

Mariko Harada-Shiba, Atsuko Takagi, Kousuke Marutsuka, Sayaka Moriguchi, Hiroaki Yagyu, Shun Ishibashi, Yujiro Asada, Shinji Yokoyama

Abstract—We previously characterized the patients with autosomal recessive hypercholesterolemia (ARH) as having severe hypercholesterolemia and retarded plasma low-density lipoprotein (LDL) clearance despite normal LDL receptor (LDLR) function in their cultured fibroblasts, and we identified a mutation in the *ARH* locus in these patients. ARH protein is an adaptor protein of the LDL and reportedly modulates its internalization. We developed ARH knockout mice ($ARH^{-/-}$) to study the function of this protein. Plasma total cholesterol level was higher in $ARH^{-/-}$ mice than that in wild-type mice ($ARH^{+/+}$), being attributed to a 6-fold increase of LDL, whereas plasma lipoprotein was normal in the heterozygotes ($ARH^{+/-}$). Clearance of ^{125}I-LDL from plasma was retarded in $ARH^{-/-}$ mice, as much as that found in $LDLR^{-/-}$ mice. Fluorescence activity of the intravenously injected 1,1′-dioctadecyl-3,3,3′,3′-tetramethylindocarbocyanine perchlorate (DiI)-LDL was recovered in the cytosol of the hepatocytes of $ARH^{+/+}$ mice, but not in those of $ARH^{-/-}$ or $LDLR^{-/-}$ mice. Also, less radioactivity was recovered in the liver of $ARH^{-/-}$ or $LDLR^{-/-}$ mice when [^{3}H]cholesteryl oleyl ether (CE)-labeled LDL was injected. In contrast, uptakes of [^{3}H]CE-labeled LDL, ^{125}I-LDL, and DiI-LDL were all normal or slightly subnormal when the $ARH^{-/-}$ hepatocytes were cultured. We thus concluded that the function of the hepatic LDLR is impaired in the $ARH^{-/-}$ mice in vivo, despite its normal function in vitro. These findings were consistent with the observations with the ARH homozygous patients and suggested that certain cellular environmental factors modulate the requirement of ARH for the LDLR function. **(*Circ Res.* 2004;95:945-952.)**

Key Words: autosomal recessive hypercholesterolemia ■ knockout mouse ■ low-density lipoprotein receptor ■ primary cultured hepatocytes ■ OmniBank

Hereditary hypercholesterolemia was first characterized by Khachadurian and Kuthman in 1973[1] as severe hypercholesterolemia with cutaneous and tendon xanthomas and premature atherosclerosis. They proposed two categories, autosomal dominant and recessive.[1] Hypercholesterolemia with autosomal dominant inheritance was termed familial hypercholesterolemia. Studies of familial hypercholesterolemia led to the discovery of low-density lipoprotein receptor (LDLR) and identification of its genetic dysfunction as the cause of this disease. The LDLR is now known to play a key role in the internalization of LDL into the cell and in the regulation of plasma LDL concentrations.[2,3] However, hypercholesterolemia with autosomal recessive inheritance had never been fully characterized until we first reported this disease.[4,5] In these articles, we described siblings with severe hypercholesterolemia, exhibiting huge xanthomas and premature atherosclerosis despite normal LDLR activity in their cultured fibroblasts.

In 2001, Garcia et al[6] mapped the *ARH* locus to chromosome 1p35 using six families of autosomal recessive hypercholesterolemia (ARH). They identified six mutations of the gene encoding a putative LDLR adaptor protein in these ARH families. We showed that an insertion mutation in the *ARH* gene of the Japanese siblings described causes an early stop codon.[7]

ARH protein has an N-terminal phosphotyrosine-binding (PTB) domain.[6] The PTB domain is found in several adaptor proteins, such as Disabled-2 and numb, and binds to an NPXY sequence in the cytoplasmic tails of cell surface receptors to modulate their internalization. Recently, the PTB domain of ARH protein was shown by the pull-down technique to bind to the FDNPVY sequence of LDLR.[8] ARH protein was also reported to interact with clathrin and is thought to function as an adaptor protein that couples LDLR to the endocytic machinery.[8]

What is unique about the patients with ARH is the apparent inconsistency of the LDLR functions between in vitro and in

Original received October 24, 2003; resubmission received June 10, 2004; revised resubmission received September 13, 2004; accepted September 24, 2004.

From the Department of Bioscience (M.H.-S.), Department of Pharmacology (A.T.), National Cardiovascular Center Research Institute, Osaka; First Department of Pathology (K.M., S.M., Y.A.), Miyazaki Medical College, Miyazaki; Division of Endocrinology and Metabolism (H.Y., S.I.), Jichi Medical School, Kawachi-gun, Tochigi; Department of Biochemistry, Cell Biology, and Metabolism (S.Y.), Nagoya City University Graduate School of Medical Sciences, Mizuho-cho, Nagoya, Aichi, Japan.

Correspondence to Mariko Harada-Shiba, Department of Bioscience, National Cardiovascular Center Research Institute, Fujishiro-dai, Suita, Osaka 565-8565, Japan. E-mail mshiba@ri.ncvc.go.jp

Circulation Research is available at http://www.circresaha.org DOI: 10.1161/01.RES.0000146946.78540.46

vivo. In ARH patients, clearance of ^{125}I-LDL from plasma is delayed to the same extent as that found among homozygous familial hypercholesterolemia, whereas LDL binding, internalization, and degradation are normal or subnormal in their cultured fibroblasts.[9–11] However, a defect in LDLR internalization was observed in Epstein-Barr virus lymphocytes from ARH patients.[12] LDLR activity in these mutant cells could be restored by retrovirus-mediated expression of normal ARH.[13] The results indicated that lymphocytes require ARH for normal functioning of the LDLR even in vitro, whereas fibroblasts express the normal LDLR functions without ARH, at least in vitro. Because ARH patients have delayed clearance of LDL, the LDLR requires ARH for its functions, at least in the liver in vivo. Jones et al[14] reported that ARH-deficient mice have delayed catabolism of LDL, higher LDL cholesterol levels, and greater immunodetectable LDLR on the sinusoidal surface of hepatocytes.

In the present study, we characterized *ARH*-deficient mice to study the functions of ARH. *ARH*$^{-/-}$ mice showed a higher level of plasma LDL cholesterol than wild-type mice, whereas *ARH*$^{+/-}$ mice did not show hypercholesterolemia, being consistent with clinical manifestation of the human ARH patients.[5,7] The clearance of ^{125}I-LDL was delayed, and hepatic uptake of 1,1′-dioctadecyl-3,3,3′,3′-tetramethylindocarbocyanine perchlorate (DiI)-LDL and of [^{3}H]cholesteryl oleyl ether-labeled LDL (^{3}H-CE-LDL) was decreased in *ARH*$^{-/-}$ mice. However, primary cultured hepatocytes of *ARH*$^{-/-}$ mice had normal functions to internalize ^{3}H-CE-LDL, ^{125}I-LDL, and DiI-LDL. Thus, the results indicate that the cellular environment modulates the regulation of LDLR function by ARH protein.

Materials and Methods

General Procedure

Plasma lipoproteins were analyzed by high-performance liquid chromatography using molecular sieve columns (Skylight Biotech, Inc).[15] Cholesterol and triglycerides were measured using enzyme assay kits (Wako, Tokyo, Japan). Na^{125}I (37 GBq/mL) and [1α,2α(*n*)-^{3}H]cholesteryl oleyl ether (^{3}H-CE) (1.63 TBq/mmol) were purchased from Amersham (Buckinghamshire, UK). LDL was isolated by sequential ultracentrifugation in a density range of 1.019<density<1.064 from pooled plasma of apolipoprotein E knockout mice (Jackson Laboratory, Bar Harbor, Me) or normal human volunteers after overnight fasting. Human lipoprotein-deficient serum (LPDS) (density>1.215 g/mL) was prepared by ultracentrifugation.

Generation of Knockout Mouse

To generate *ARH* knockout mice, mutations were created by insertional mutagenesis using the gene trap vectors developed by Lexicon Genetics Incorporated (Woodlands, Tex), based on retroviral-based gene trap technology previously reported.[16] OmniBank Sequence Tag 149604 corresponded to the insertion mutation in the third intron of *ARH* gene in mouse chromosome 4 (Figure 1A). The line was obtained from Lexicon Genetics Incorporated. All experiments were performed with the F2-generation or F3-generation descendants, which were backcrossed with the C57Bl/6. LDLR knockout mice (*LDLR*$^{-/-}$) were generated as previously described,[17] which were backcrossed to C57Bl/6 mice, and were used for the study.

Southern Blot Analysis

Southern blot analysis was performed after digestion of the DNA prepared from liver with *Apa*I. ^{32}P-labeled polymerase chain reaction products (239 bp) amplified from portions of exon 3 and intron 3 of the mouse *ARH* gene with primers 5′-ATCATCCTGACCGACAGCCT-3′ and 5′-GGCACAACATAACCGACCTA-3′ or neo gene fragment (850 bp) derived from pBS64neo (Lexicon Genetics Inc) as probes according to the standard procedure.[18]

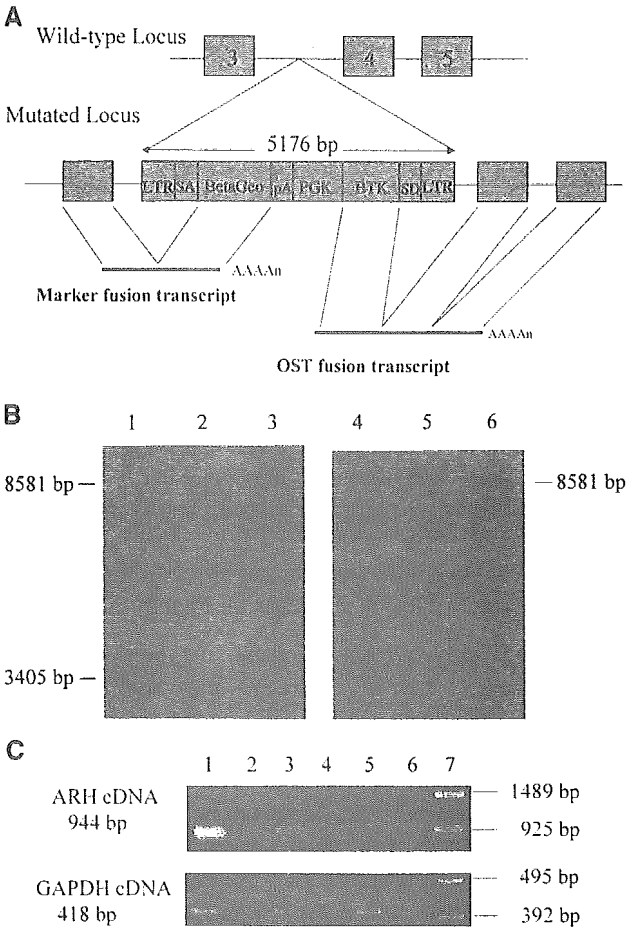

Figure 1. A, Strategy for insertional mutagenesis of the *ARH* locus in the mouse genome. The gene trap vector contains a promoterless splice acceptor sequence (SA) and BetaGeo, which create marker fusion transcripts. The vector also contains a long terminal repeat (LTR), a phosphoglycerate kinase-1 promoter (PGK), Bruton tyrosine kinase (BTK), and a splice donor sequence (SD). OmniBank Sequence Tag 149604 has an insertion of the vector in the third intron of *ARH* gene. B, Southern blot analysis of liver DNA. DNA was digested with *Apa*I and hybridized with a probe comprising portions of the mouse *ARH* gene containing exon 3 and intron 3 (lanes 1 to 3) or neo gene (lanes 4 to 6). Lanes 1 and 4, *ARH*$^{+/+}$; lanes 2 and 5, *ARH*$^{+/-}$; lanes 3 and 6, *ARH*$^{-/-}$. C, Reverse-transcription polymerase chain reaction of ARH and GAPDH mRNA. Lane 1 and 2, *ARH*$^{+/+}$; 3 and 4, *ARH*$^{+/-}$; 5 and 6, *ARH*$^{-/-}$. Lane 1, 3, and 5 are reverse-transcription plus; 2, 4, and 6 are reverse-transcription minus. Lane 7 shows size markers, lambda DNA digested with *Sty*1 for ARH, and phiX174 DNA digested with *Hin*cII for GAPDH.

Reverse-Transcription Polymerase Chain Reaction

Total RNA was isolated from the liver of wild-type, heterozygous, and homozygous mice using the acid guanidium thiocyanate-phenol-chloroform method, as described.[19]

^{125}I-LDL Turnover Study

Mouse LDL was iodinated with ^{125}I by the iodine monochloride method[20] to give a specific activity of ^{125}I-LDL >200 cpm/ng

protein. Female mice of the genotypes of wild-type ($ARH^{+/+}$), $ARH^{+/-}$, $ARH^{-/-}$, and $LDLR^{-/-}$, 12 to 15 weeks of age, were fasted for 13 hours. Three mice in each genotype received an intravenous bolus via the external jugular vein of ^{125}I-labeled mouse LDL (5 μg of protein). Blood was collected from the tail vein with heparinized Pasteur pipette at the indicated timings. The plasma ^{125}I-labeled apoB was measured by isopropanol precipitation, followed by gamma counting as previously described.[17]

In Vivo Hepatic Uptake of Intravenously Injected DiI-LDL

Twelve-week-old female mice of the genotypes of wild-type, $ARH^{-/-}$, and $LDLR^{-/-}$ were fasted for 13 hours. Each mouse received an intravenous bolus via the external jugular vein of 50 μg of human DiI-LDL (Molecular Probes Inc, Eugene, Ore). To detect nonspecific incorporation of DiI-LDL, 2.5 mg of unlabeled human LDL was injected 2 minutes before 50 μg of DiI-LDL was injected. Two minutes after DiI-LDL injection, blood was collected for determination of cholesterol and lipoproteins. After 4 hours, the right atrium was punctured, 10 mL of phosphate-buffered saline (PBS) was injected via the left ventricle, and subsequently 10 mL of PBS containing 4% paraformaldehyde. The tissues were immersed in PBS containing 4% paraformaldehyde at 4°C for 12 hours. The liver samples were frozen in liquid nitrogen and subjected to microscopic analysis. To stain Kupffer cells, BM8 (rat antibody against mouse pan-macrophage) (BMA Biomedicals AG, Augst, Switzerland) was used as a primary antibody and fluorescein isothiocyanate-conjugated rabbit anti-rat IgG (DAKO Cytomation, Glostrup, Denmark) was used as a secondary antibody. The samples were observed by confocal laser scanning microscopy (LSM5 PASCAL; Zeiss, Co, Tokyo, Japan).

Labeling of Human LDL With ^{3}H-CE

LDL was labeled with ^{3}H-CE according to the previously described method,[21] with a minor modifications.

In Vivo Hepatic Uptake of Intravenously Injected ^{3}H-CE-LDL

^{3}H-CE-LDL (0.8 μCi) was injected via the external jugular vein of wild-type ($ARH^{+/+}$), $ARH^{-/-}$, and $LDLR^{-/-}$ female mice, 12 to 15 weeks of age. Blood was collected from the tail vein with heparinized Pasteur pipette at 2 minutes and 4 hours after the injection. The blood was dispersed in chloroform/methanol, 2/1 (v/v). Immediately after the second blood collection, 2 mg of human LDL was injected via the inferior vena cava. Ten minutes later, the right atrium was punctured and 20 mL of PBS was injected via the left ventricle three times to wash the blood from the body. The liver was isolated, immersed in chloroform/methanol 2/1 (v/v), and homogenized with a polytron homogenizer. The lipid was extracted from the liver and the blood by the method of Folch.[22] Radioactivity in each sample was counted in a liquid scintillation counter using a scintillation cocktail of toluene/Triton X100 (2:1) containing PPO (0.6%) and POPOP (0.05%).

Preparation and Culture of Mouse Hepatocytes

Mice (14 to 16 weeks of age) of the indicated genotype were used for the study. The livers were perfused via the portal vein and hepatocytes were obtained by the method of Seglen.[23] After 24-hour incubation in Waymouth MB 752/1 medium containing 10% fetal calf serum in six-well plates, the cells were subjected to the study.

In Vitro Uptake of ^{3}H-CE-LDL Into Primary Cultured Hepatocytes

The cells were incubated in Waymouth MB 752/1 medium containing 10% LPDS for 48 hours, and then incubated in DMEM containing 2% bovine serum albumin (without free fatty acid) and ^{3}H-CE-LDL (5 to 100 μg/mL) for an additional 3 hours. Then, the cells were washed twice with 150 mmol/L NaCl, 50 mmol/L of Tris-HCl (pH 7.4) containing 2 mg/mL of bovine serum albumin, and once with the same buffer without bovine serum albumin. The cells were incubated with LDL-releasing buffer (50 mmol/L NaCl, 10 mmol/L Hepes (pH 7.4), containing 10 mg/mL heparin) at 4°C for 1 hour. After removal of the heparin-releasable fraction, 1 mL of hexane/isopropyl alcohol (3/2) was added to the cells to extract lipids in the cells.[24] After delipidation, the cells were dissolved in 1 N NaOH and protein concentration was measured.

^{125}I-LDL Binding, Incorporation, and Degradation Assays

Waymouth MB 752/1 medium containing 10% LPDS was added to the cells and incubated for another 24 hours. Binding, internalization, and degradation of ^{125}I-LDL were analyzed according to the method previously described.[25]

DiI-LDL Incorporation Into Primary Cultured Hepatocytes

The cells were added to Waymouth MB 752/1 medium containing 10% LPDS and incubated for 24 hours. Then, the cells were washed twice and incubated at 37°C for 3 hours with 50 μg/mL of DiI-LDL in 0.2 mL of MEM containing 10% LPDS. Nonspecific incorporation was determined by parallel incubation in the presence of 20-fold excess of LDL. The cells were washed three times with PBS containing 0.2% bovine serum albumin, followed by washing twice with PBS. The samples were observed with a laser confocal microscopy.

An expanded Materials and Methods section is available in the online data supplement at http://circres.ahajournals.org.

Results

Generation of *ARH* Knockout Mice

OmniBank Sequence Tag 149604 (Lexicon Genetics Inc) corresponded to the insertion mutation in the third intron of *ARH* gene in mouse chromosome 4 (Figure 1A). The mutated allele encodes a marker fusion transcript and OmniBank Sequence Tag fusion transcript instead of *ARH* mRNA. The offspring heterozygous animals were mated to produce $ARH^{+/+}$, $ARH^{+/-}$, and $ARH^{-/-}$ mice. Southern blot analysis was performed to genotype the mice using a probe comprising portions of mouse *ARH* gene containing both exon 3 and intron 3 (Figure 1B) after digestion of DNA with *Apa*I. *Apa*I site is not present in the insertion fragment used for development of the knockout mice. Southern blot analysis with the exon probe showed a 3405-bp band for the wild-type allele and was observed in both the wild-type and $ARH^{+/-}$ mice, whereas an 8581-bp band, the disrupted allele which was produced by the insertion of 5176-bp fragment (Figure 1A), was observed in $ARH^{+/-}$ and $ARH^{-/-}$ mice after digestion of DNA with *Apa*I. Southern blot analysis with neo gene probe demonstrated that only one position and one copy insertion event occurred in a mouse genome because $ARH^{+/-}$ and $ARH^{-/-}$ exhibited an 8581 bp.

To confirm that the mutated allele does not express the mRNA, total RNA was isolated from the livers of the animals of each genotype and analyzed by reverse-transcription polymerase chain reaction (Figure 1C). A 944-bp band, the *ARH* transcript that was expressed in wild-type and $ARH^{+/-}$mice, was not detectable in $ARH^{-/-}$ mice. The results thus confirmed that the insertion mutation by gene trap vector disrupted the *ARH* gene expression.

TABLE 1. Lipid and Lipoprotein Profiles of ARH Knockout Mice (mean±SEM)

	Total Cholesterol, mmol/L	Triglyceride, mmol/L	HDL Cholesterol, mmol/L	LDL Cholesterol, mmol/L
Wild type				
Male (n=5)	2.68±0.14	1.04±0.26	2.49±0.12	0.17±0.05
Female (n=8)	2.57±0.22	0.78±0.07	2.20±0.19	0.30±0.04
Heterozygote				
Male (n=8)	2.92±0.14	1.00±0.13	2.78±0.11	0.13±0.03
Female (n=10)	2.82±0.19	0.76±0.06	2.40±0.14	0.35±0.08
Homozygote				
Male (n=5)	4.53±0.35†	1.20±0.10	3.10±0.52	1.01±0.21†
Female (n=8)	4.64±0.68†	1.09±0.19	2.96±0.30*	1.46±0.44*

*$P<0.05$.
†$P<0.01$ vs wild type.

Lipid and Lipoprotein Profiles of *ARH* Knockout Mice

Table 1 shows total plasma cholesterol, triglycerides, LDL cholesterol, and HDL cholesterol levels of mice from litters derived from the mating of $ARH^{+/-}$ mice fed a normal chow. Plasma total cholesterol levels were 1.8-fold higher in $ARH^{-/-}$ mice than those in $ARH^{+/+}$. The elevation of total cholesterol was attributed to the six-fold increase of LDL cholesterol. There was no significant difference in the plasma cholesterol levels between $ARH^{+/-}$ and $ARH^{+/+}$ mice. Histological analysis of the liver showed that $ARH^{-/-}$ mice at 12 weeks of age did not have fatty livers, which were observed in our ARH patients.[5]

^{125}I-LDL Turnover Study

To investigate the LDL metabolism in ARH deficiency, ^{125}I-LDL turnover study was performed in $ARH^{-/-}$, $ARH^{+/-}$, $ARH^{+/+}$ (wild-type), and $LDLR^{-/-}$ mice. The clearance of ^{125}I-LDL from circulation is demonstrated in a semilogarithmic plot in Figure 2. It was substantially retarded in $ARH^{-/-}$ and $LDLR^{-/-}$ mice compared with wild-type mice. The clearance rate of ^{125}I-LDL in $ARH^{+/-}$ mice was similar to that in wild-type mice. The half-lives of the plasma ^{125}I-LDL were 11.7 hours in $ARH^{-/-}$ and 6.0 hours in $LDLR^{-/-}$ mice, and both were longer than those in $ARH^{+/-}$ and wild-type mice (2.8 hours).

Microscopic Findings in the Liver After Injection of DiI-LDL

To study whether the delayed clearance of LDL in $ARH^{-/-}$ mice is attributable to impaired catabolism of LDL in the liver, the liver specimen was examined after injection of DiI-LDL in wild-type, $LDLR^{-/-}$, and $ARH^{-/-}$ mice (Figure 3). Kupffer cells were identified by fluorescein isothiocyanate (Figure 3B, 3D, 3F, 3H, 3J, and 3L). Fluorescence activity was detected in the cytosol of the hepatocytes and Kupffer cells in wild-type mice, indicating that both types of cells effectively take-up DiI-LDL (Figure 3A). Pre-injection of 2.5 mg LDL raised serum total cholesterol from 2.18±0.66 (mean±SD) mmol/L to 14.67±0.68 mmol/L, and LDL cholesterol from 0.21±0.07 mmol/L to 11.42±1.09 mmol/L in wild-type mice (Table 2). In this condition, the incorporation

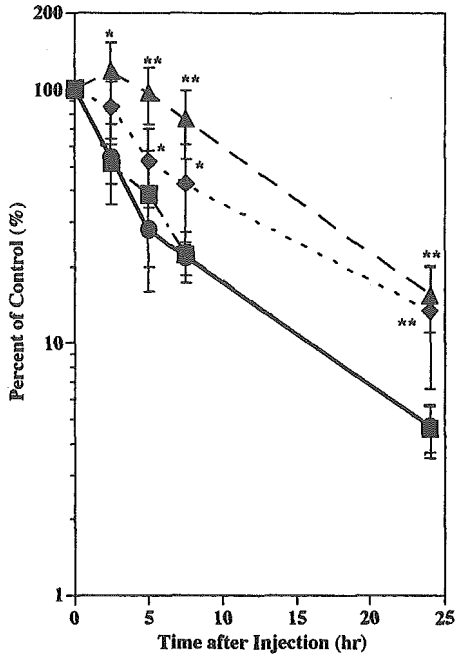

Figure 2. ^{125}I-LDL turnover study of wild-type (●), $ARH^{+/-}$ (■), $ARH^{-/-}$ (▲), and $LDLR^{-/-}$ (◆) mice. After 13 hours of fasting, wild-type, $ARH^{+/-}$, $ARH^{-/-}$, and $LDLR^{-/-}$ mice (three of each) were injected with 5 μg of ^{125}I-LDL. After the indicated time, blood was collected from the tail vein. The plasma content of ^{125}I-labeled apoB was measured by isopropanol precipitation, followed by gamma counting. The data are shown in semilogarithmic plots, and each data point represents the mean±SEM for triplicate assay. *$P<0.05$, **$P<0.01$.

of DiI-LDL into hepatocytes was decreased by the excess amount of LDL in plasma (Figure 3C), whereas its incorporation into Kupffer cells was not affected. In contrast, hepatocytes of $ARH^{-/-}$ mice were stained less extensively than those of wild-type mice by DiI-LDL fluorescence (Figure 3I), indicating that the uptake of DiI-LDL by the hepatocytes of $ARH^{-/-}$ mice was smaller than that of wild-type mice, and the presence of excess amount of LDL in plasma did not influence this result (Figure 3K). The fluorescence in the hepatocytes of $LDLR^{-/-}$ mice was also less intense than that in $ARH^{-/-}$ (Figure 3E).

In Vivo Hepatic Uptake of Intravenously Injected ^{3}H-CE-LDL

Hepatic uptake of LDL was also investigated by injecting ^{3}H-CE-LDL. Four hours after the injection, the tritium count in the blood decreased by 44% in wild-type mice, whereas it did not decrease in either $LDLR^{-/-}$ or $ARH^{-/-}$ mice (Figure 4A). The liver of wild-type mice incorporated 27.4±8.0% (mean±SD) of the injected ^{3}H-CE-LDL, whereas 9.0±1.0% was incorporated in $LDLR^{-/-}$ mice and 11.8±0.5% in $ARH^{-/-}$ mice (Figure 4B). The amount of ^{3}H-CE-LDL taken-up by the liver in $ARH^{-/-}$ was significantly smaller than that in wild-type mice but larger than that in $LDLR^{-/-}$ mice ($P<0.05$).

Incorporation of LDL in Primary Cultured Hepatocytes

In an attempt to reproduce the in vivo observations in vitro, incorporation of ^{3}H-CE-LDL was examined in primary cul-

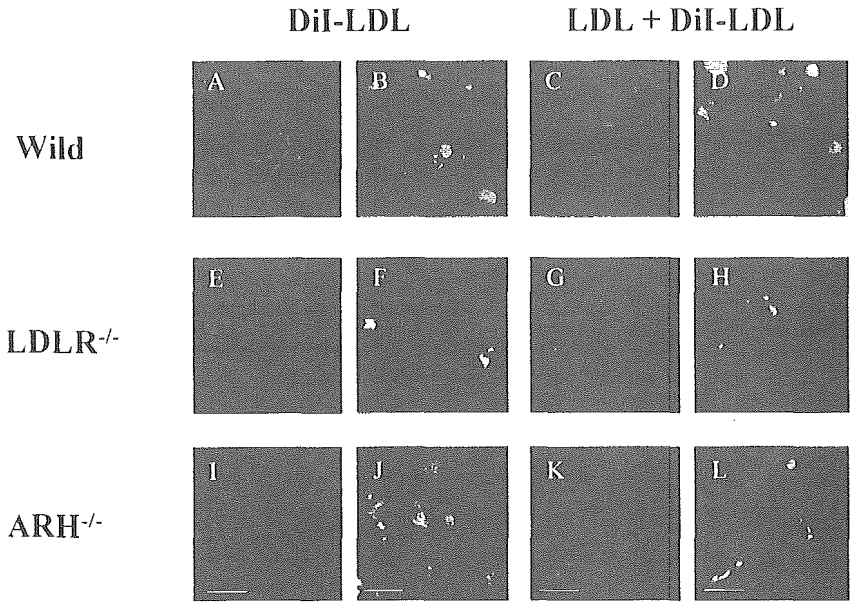

Figure 3. Microscopic findings of the liver after injection of DiI-LDL. A, E, and I, The liver from a mouse of each genotype 4 hours after the injection of 50 μg of DiI-LDL. C, G, and K, The liver from a mouse of each genotype, 4 hours after the injection of 2.5 mg of LDL, followed by 50 μg of DiI-LDL. B, F, and J, The liver from a mouse of each genotype, 4 hours after the injection of 50 μg of DiI-LDL. The specimens were stained with rat anti-mouse pan-macrophage antibody. D, H, and L, The liver from each genotype of mouse 4 hours after injection of 2.5 mg of LDL, followed by 50 μg of DiI-LDL. The specimen was stained with rat anti-mouse pan-macrophage antibody. The scale bar indicates 20 μm.

tured hepatocytes. Interestingly, the hepatocytes of *ARH*$^{-/-}$ mice internalized ^{3}H-CE-LDL as much as those of wild-type mice, whereas the hepatocytes of *LDLR*$^{-/-}$ mice took-up significantly less ^{3}H-CE-LDL (Figure 5A). The cultured hepatocytes of *ARH*$^{-/-}$ mice bound larger amounts of ^{125}I-LDL than those of wild-type and *LDLR*$^{-/-}$ mice. The hepatocytes of *ARH*$^{-/-}$ internalized and degraded ^{125}I-LDL as much as those of wild-type mice, which was significantly more than those of *LDLR*$^{-/-}$ mice (Figure 5B through 5D).

DiI-LDL Incorporation in Primary Cultured Hepatocytes

To confirm the positive incorporation of LDL by the primary cultured hepatocytes without ARH, the hepatocytes of *ARH*$^{-/-}$, *LDLR*$^{-/-}$, and wild-type mice were incubated with DiI-LDL and were observed by a laser confocal microscopy. Fluorescence-positive substances were observed in the cytosol of the hepatocytes of wild-type mice (Figure 6A), and they were suppressed in the presence of excess amounts of LDL (Figure 6B). The cultured hepatocytes of *LDLR*$^{-/-}$ mice showed very low fluorescence activity (Figure 6C and 6D). In contrast, the hepatocytes of *ARH*$^{-/-}$ mice showed fluorescence uptake of amounts similar to those observed for the wild-type (Figure 6E), and this was efficiently suppressed by excess amounts of LDL (Figure 6F).

TABLE 2. Cholesterol Levels of Total, VLDL, LDL, and HDL Fractions Before and After Administration of 2.5 mg LDL

	Total Cholesterol, mmol/L		VLDL Cholesterol, mmol/L		LDL Cholesterol, mmol/L		HDL Cholesterol, mmol/L	
	Before	After	Before	After	Before	After	Before	After
Wild-1	2.36	14.30	0.02	1.99	0.12	10.56	2.22	1.74
Wild-2	2.72	14.27	0.05	1.37	0.24	11.04	2.44	1.86
Wild-3	1.45	15.45	0.06	2.10	0.26	12.64	1.13	0.71
Mean	2.18	14.67	0.04	1.82	0.21	11.42	1.93	1.43
SD	0.66	0.68	0.02	0.39	0.07	1.09	0.70	0.63

VLDL indicates very-low-density lipoprotein.

Discussion

ARH knockout mice were developed by insertion mutation in the third intron of mouse chromosome 4. *ARH*$^{-/-}$ mice had a 1.8-fold higher plasma total cholesterol than wild-type litter mates fed normal chow, and this was attributed to a six-fold increase of LDL. Total cholesterol levels in *ARH*$^{-/-}$ mice (Table 1) were slightly lower than those reported for *LDLR*$^{-/-}$ mice (5.90±0.23 mmol/L in male, 6.18±0.21 mmol/L in female),[17] and cholesterol levels in *ARH*$^{+/-}$ mice (2.92±0.14 mmol/L in male, 2.82±0.19 mmol/L in female) were almost the same as those in *ARH*$^{+/+}$ mice (2.68±0.14 mmol/L in male, 2.57±0.22 mmol/L in female). The hypercholesterolemia in our *ARH*$^{-/-}$ mice appears to be milder than that reported by Jones et al,[14] who have recently reported that total cholesterol levels were moderately higher both in *ARH*$^{-/-}$ mice (7.96±1.63 mmol/L) and in *ARH*$^{+/-}$ mice (4.06±0.58 mmol/L) compared with that in *ARH*$^{+/+}$ mice (3.26±1.00 mmol/L) fed a chow containing 0.2% cholesterol. The difference in the plasma total cholesterol values between our *ARH*$^{-/-}$ mice and theirs may stem from different cholesterol content of the diet, because the chow we used contained 0.1% cholesterol.

The clearance of ^{125}I-LDL from the circulation was significantly delayed in *ARH*$^{-/-}$ mice like in *LDLR*$^{-/-}$ mice (Figure 2), indicating that the in vivo catabolic rate of LDL is decreased in *ARH*$^{-/-}$ mice. The half-life for the disappearance of ^{125}I-LDL in *ARH*$^{-/-}$ mice (11.7 hours) was longer than that observed in wild-type mice (2.8 hours) but not significantly different from that in *LDLR*$^{-/-}$ (6.0 hours). The LDL clearance in *ARH*$^{-/-}$ mice was same as that in the wild-type mice, suggesting that their LDL catabolism is normal. These results appear to be consistent with the findings in the ARH patients.[5]

To investigate the in vivo mechanism for the delayed catabolism of LDL directly in *ARH*$^{-/-}$ mice, hepatic uptake of